https://doi.org/10.5194/gmd-2021-23
Preprint. Discussion started: 20 April 2021

Geoscientific Model Development Discussions
Open Access
EGU

Integrating Agricultural Practices into the TRIPLEX-GHG Model v2.0 for Simulating Global Cropland Nitrous Oxide Emissions: Model Development and Evaluation

Hanxiong Song[1,2], Changhui Peng[1,2]*, Kerou Zhang[3], and Qiuan Zhu[4]

1.Department of Biology Sciences, University of Quebec at Montreal, C.P. 8888, Succ. Center-Ville, Montreal H3C 3P8, Canada

2. Center for Ecological Forecasting and Global Change, College of Forestry, Northwest A&F University, Yangling, China

3. Institute of Wetland Research, Chinese Academy of Forestry, Beijing, China

4. College of Hydrology and Water Resources, Hohai University, Nanjing, China

Correspondence to: Changhui Peng (peng.changhui@uqam.ca)

https://doi.org/10.5194/gmd-2021-23
Preprint. Discussion started: 20 April 2021

Geoscientific Model Development Discussions

Abstract Nitrous oxide (N_2O) emissions from croplands are one of the most important greenhouse gas sources, and it is difficult to simulate on a large scale. In order to simulate N_2O emissions from global croplands, a new version of the process-based TRIPLEX-GHG model was developed by coupling the major agricultural activities. The coefficient of the NO_3^- consumption rate for denitrification (COE_{dNO3}) was found to be the most sensitive parameter based on sensitivity analysis, and it was calibrated using field data from 39 observation sites across major croplands globally. The model performed well when simulating the magnitude of the daily N_2O emissions and was able to capture the temporal patterns of the N_2O emissions. The COE_{dNO3} ranged from 0.01 to 0.05, and the continental mean of the parameter was used for the model validation. The validation results indicate that the means of the measured daily N_2O fluxes during the experiment periods are highly correlated with the modeled results (R^2 = 0.87). Consequently, our model simulation results demonstrate that the new version of the TRIPLEX-GHG model can reliably simulate N_2O emissions from various croplands at the global scale.

Key Words: N_2O, croplands, process-based model, fertilization

https://doi.org/10.5194/gmd-2021-23
Preprint. Discussion started: 20 April 2021

1. Introduction

Nitrous oxide (N_2O) is a long-lived trace gas that has a global warming potential on a 100-year time horizon that is 265–298 times larger than that of carbon dioxide (CO_2), and it simultaneously results in ozone depletion in the stratosphere (Ciais et al., 2014). The atmospheric concentration of N_2O has significantly increased (i.e., by 20%) since the industrial revolution (Tian et al., 2016; Tian et al., 2020). Generally, N_2O is produced as an intermediate product of soil microbial nitrification and denitrification processes and is regulated by multiple biotic (i.e., vegetation type, microbial biomass) and abiotic factors (i.e., climate, soil temperature, humidity, nutrient content, and texture) (Bouwman et al., 2002; Stehfest and Bouwman, 2006; Li et al., 2000; Butterbach-Bahl et al., 2013; Tian et al., 2018).

Cropland is a hotspot of terrestrial N_2O sources (Tian et al., 2019; Tian et al., 2020). The current larger emission rate of cropland soil comparing with natural soil (Davidson and Kanter, 2014) results from extensive agricultural practices, including N-fertilizer input (synthetic and manure) (Davidson, 2009; Zhou et al., 2017), irrigation (Li et al., 2000; Li et al., 2010), and tillage (Powlson et al., 2014; Mei et al., 2018), because these agricultural practices directly and indirectly interfere with soil N flow and microbial activities (Cavigelli et al., 2012). Therefore, substantial observation studies have been conducted in croplands to understand the effects of different agricultural practices on N_2O emissions in order to enable sustainable agricultural production (Carlson et al., 2017; Burney et al., 2010; Snyder et al., 2009). However, because of the characteristics of the varying magnitudes across the study sites and periods (Tian et al., 2016; Tian et al., 2019), the emission pattern of N_2O requires models to be quantitatively investigated on large scales (Li et al., 2000; Wrage et al., 2001; Tian et al., 2018).

Modeling is an important approach for quantifying the N_2O emissions from various ecosystems, especially croplands, under changing environments and management. Linear and non-linear models based on emission factors (EF) have been widely used to estimate direct N_2O emissions on different scales (Shcherbak et al., 2014; Davidson, 2009; Gerber et al., 2016; Hoben et al., 2011). However, the EF method has been questioned due to the large uncertainty generated by its inability to depict spatial (i.e., site, regional and global) and temporal (i.e., monthly, daily) variations (Ehrhardt et al., 2018; Tian et al., 2019; Berdanier and Conant, 2012). Models based on machine learning algorithms such as the random forest algorithm (Philibert et al., 2013), artificial neural network (Oehler et al., 2010), and Bayesian inversion (Berdanier and Conant, 2012) have recently been applied to cropland N_2O emission estimations, but these methods strongly depend on the quality of the training data, instead of the underlying mechanism of the N_2O-related processes.

Process-based biogeochemical models, which serve as an alternative, have been demonstrated to be an effective tool for assessing and predicting the N_2O flux by describing the N_2O emission processes and dynamics and by integrating the natural and anthropogenic drivers at different scales (Tian et al., 2019; Tian et al., 2018). The DAYCENT (Daily Century) model has provided adequate simulations of N_2O fluxes for a variety of agroecosystems with different scales (Del Grosso et al., 2005; Cheng et al., 2014; Del Grosso et al., 2009; Alvaro-Fuentes et al., 2017). Nevertheless, because it predominately utilizes simple

https://doi.org/10.5194/gmd-2021-23
Preprint. Discussion started: 20 April 2021


Geoscientific Model Development Discussions

functions based on soil water, inorganic nitrogen (N) concentrations, respiration, and texture (Del Grosso et al., 2000; Parton et al., 1996), the limited model descriptions for oxygen diffusion and consumption processes lead to relatively large uncertainties, especially for disturbed soils (Butterbach-Bahl et al., 2013; Alvaro-Fuentes et al., 2017; Song et al., 2019). The Carnegie-Ames-Stanford (CASA) biosphere model estimates the soil N_2O flux based on the concept of the "hole in a pipe model" (Potter et al., 1996), but the lack of a detailed description of the microbial activities limits the model's performance (Li et al., 2020). Tian et al. (2010) developed a process-based biogeochemical model, i.e., the Dynamic Land Ecosystem Model (DLEM), which has been successfully used to estimate N_2O emissions at continental and global scales (Tian et al., 2010; Xu et al., 2017). However, due to the absence of the effect of soil pH, the nitrification and denitrification processes were simulated based on empirical models (Chatskikh et al., 2005; Heinen, 2006), which might be responsible for the bias of the modeled results. The DeNitrification-DeComposition (DNDC) model, developed by Li et al. (1992), which is a well-known process-based model, has been widely used to estimate N_2O emissions and crop production in agroecosystems on site to regional scales (Li et al., 2000; Giltrap et al., 2010; Lugato et al., 2010). However, the proper application of the DNDC requires relatively complex agricultural practices as input information, which limits its large-scale modeling ability (Perlman et al., 2014). Furthermore, dynamic global vegetation models (DGVM) have also been coupled with N_2O-related processes. Because of the advantage that they reflect the vegetation response to climate change, DGVMs are capable of simulating N_2O emissions on a global scale (Saikawa et al., 2013; Xu and Prentice, 2008; Xu et al., 2012; Zhang et al., 2017b). For instance, Xu-Ri et al. (2012) successfully developed the DyN-LPJ model to estimate the total N_2O emissions from the global terrestrial ecosystem. However, by only integrating simple semi-empirical equations without the complex, subsidiary processes of the N_2O dynamics, the DyN-LPJ model has not been used to simulate N_2O emissions from fertilized agricultural soils or soils with any other anthropogenic effects (Xu et al., 2012; Xu and Prentice, 2008).

The global N_2O Model Intercomparison Project (NMIP) has compared the modeled N_2O emissions from global terrestrial ecosystems simulated using 10 process-based biogeochemical models, and it has been reported that large uncertainties still exist in the current estimations of the global N_2O budget (Tian et al., 2018). These results have been confirmed by ensemble model studies (Ehrhardt et al., 2018; Tian et al., 2019), and the modeled uncertainties are probably generated by the large temporal and spatial variations in the N_2O flux and the differences in the model structures, parameterization schemes, and input datasets. Therefore, further improvement of process-based N_2O emission models is critical for reducing the global modeling uncertainties and for closing the global N_2O budget in order to cope with the global change.

As a recently developed process-based model, the TRIPLEX-GHG (Zhu et al., 2014) can simulate multiple ecological processes and has been successfully applied to simulate N_2O fluxes from natural ecosystems (grasslands, forests) (Zhang et al., 2017b). However, the impact of human disturbances (e.g., agricultural practices, land use changes, and management) have not been considered so far (Tian et al., 2018). In this study, we enhanced the TRIPLEX-GHG model's capability by addressing

https://doi.org/10.5194/gmd-2021-23
Preprint. Discussion started: 20 April 2021

the impacts of major agricultural practices on the N_2O production and emission processes in order to simulate N_2O emissions from global croplands. The objectives of this study were: (1) to develop agricultural practice modules in the framework of an extant process-based model (i.e., the TRIPLEX-GHG); (2) to conduct a sensitivity analysis to identify the most sensitive parameter; and (3) to validate modeled the results using field observations of various cropland sites at the global scale.

2. Model description

The TRIPLEX-GHG model (Peng et al., 2013; Zhang et al., 2017b; Zhu et al., 2014) is a process-based terrestrial ecosystem model, which is based on the Integrated Biosphere Simulator (IBIS) (Foley et al., 1996; Kucharik et al., 2000) and TRIPLEX (Peng et al., 2002). The basic structure of the original TRIPLEX-GHG model and the integration of agricultural management processes are shown in Fig. 1, and are described in detail below.

The TRIPLEX-GHG model consists of four key submodules: a land surface submodule for simulating the energy budget and hydrological cycle between the soil surface, vegetation canopy, and the atmosphere; a dynamic vegetation submodule that is used to determine the geographic distribution of specific plant functional types (PFTs) under climate change; a plant phenology submodule that describes the dominate phenological behavior of each PFT based on a set of phenological parameterizations (Botta et al., 2000); and a soil biogeochemical submodule that simulates the dynamics of the C and N flows and the major microbial processes, including nutrient mineralization, immobilization, and their interactions with the environment. Specifically, the biogeochemical processes mostly focus on the C cycle within three plant biomass pools (leaf, root, and wood, each of which can be further divided into the metabolic, structural, and lignin pool) and three soil organic matter pools (litter, humus, and microbial), which are comprised of non-protected, protected, and passive organic matter. However, the N cycle's scheme is coupled with the C cycle and relies on the corresponding C:N ratios of the different organic matter pools and two additional inorganic N pools (nitrite-N [NO_3^-] and ammonium-N[NH_4^+]).

By incorporating the decomposition, methane (CH_4) production and oxidation, nitrification, and denitrification processes with the original model, the TRIPLEX-GHG model has been validated, modified, and used to simulate major green-house gas emissions from natural terrestrial ecosystems (grasslands, forests, and wetlands) (Zhang et al., 2017b; Zhang et al., 2019; Zhu et al., 2014; Zhu et al., 2015). However, the current TRIPLEX-GHG model does not include major agricultural practices, and thus, it is unable to accurately simulate the N_2O flux from agricultural soils. To overcome this problem and reduce the uncertainties in global N_2O simulations, the main framework for improving the TRIPLEX-GHG model was to add a new component that takes into account how agricultural practices affect the biogeochemical cycle, especially the nitrification and denitrification processes, thus modifying the pattern of the N_2O flux of croplands at the global scale.

2.1 The N_2O module

https://doi.org/10.5194/gmd-2021-23
Preprint. Discussion started: 20 April 2021


Geoscientific Model Development Discussions

As a trace N gas, the N_2O emitted by nitrification and denitrification were simulated according to the anaerobic balloon concept. The anaerobic volumetric fraction (ANVF) was the key parameter, which represents the soil oxygen status and regulates the allocation rates of the substrates (e.g., dissolved soil organic carbon (DOC), NH_4^+, and NO_3^-) for nitrification and denitrification. It was calculated using the oxygen partial pressure and the air-filled porosity listed in Supporting Information Table S1 (Equations (1–3)).

In the TRIPLEX-GHG model, nitrification is an aerobic process that occurs outside of the anaerobic balloon, converting ammonium (NH_4^+) into nitrate (NO_3^-) driven by nitrifying bacteria with N_2O as a by-product (Li et al., 2000; Zhang et al., 2017b; Morkved et al., 2007). The growth and death rate of nitrifiers (Equations (4–6) in Table S1) are highly dependent on the DOC; therefore, the nitrification rate (Equations (7–10) in Table S1) was calculated using the Michaelis–Menten function based on the concentration of NH_4^+ and the microbial activity of the nitrifying bacteria. The effects of the soil properties were also simulated (Equations (11–12) in Table S1).

Denitrification is the process through which the nitrate is reduced stepwise into different nitrogen gases as a chain reaction process inside of the anaerobic balloon. Denitrification can be divided into 4 independent steps, which are linked by the competition for DOC by the specific denitrifiers during each step (Betlach and Tiedje, 1981). Similarly, the growth and mortality rates of the different denitrifiers utilized a double substrate based (DOC and NOx) Michaelis–Menten equation (Equations (13–14) in Table S1). The consumption of NO_X for the growth of the different denitrifiers was calculated at an hourly time step according to previous studies as is shown in the following Eq. (1) (Leffelaar and Wessel, 1998; Li et al., 2000):

$$F_{ANNOX} = COE_{dNOX} \cdot B_{denit} \cdot \left(\frac{R_{NOX}}{EFF_{NOX}} + \frac{MAI_{NOX} \cdot [NO_X]}{[N]}\right) \cdot f_{NOX}(pH) \cdot f(t). \quad (1)$$

Here, F_{ANNOX} is the consumption rate of NO_X (kg N m^{-3} h^{-1}); COE_{dNOX} is the coefficient of NO_X consumption; B_{denit} is the biomass of the denitrifiers (kg C m^{-3}); R_{NOX} is the NO_X reduction rate (h^{-1}); EFF_{NOX} is the efficiency of the NO_X denitrifiers (kg C kg N $^{-1}$); MAI_{NOX} is the maintenance coefficient of NO_X (h^{-1}); $[NO_X]$ and $[N]$ are the NO_X and total N concentrations in the anaerobic balloon, respectively; and $f_{NOX}(pH)$ and $f(t)$ are the effects of the soil pH and soil temperature on the NO_X denitrification rate in each step, respectively (Equations (15–17) and Equation (18) in Table S1).

In our model, all of the gaseous products of the nitrification and denitrification (N_2O primarily) are emitted from the bottom layer of the soil into the atmosphere primarily driven by diffusion based on the N_2O concentration and soil depth according to Fick's law of diffusion (Equations (19–20) in Table S1).

2.2 Effects of agricultural management practices

N_2O production and emission are key parts of the soil N cycle. These processes are controlled by the environmental conditions, which directly respond to the varying soil management practices (Butterbach-Bahl et al., 2013). Understanding the direct and indirect effects of the different agricultural practices on the soil N flow (N input and output) is critical to accurately predicting the N_2O fluxes in cropland ecosystems (Liu et al., 2010).

https://doi.org/10.5194/gmd-2021-23
Preprint. Discussion started: 20 April 2021

Geoscientific Model Development Discussions

2.2.1 N output

Except for gaseous N losses (N_2O, NO, NH_3), crop uptake/harvest processes, leaching, and surface runoff are the major N outputs (Liu et al., 2010). We altered the plant N uptake process and integrated harvest practices into the original model.

Plant N uptake: As a plant grows, mineral N is taken up as NO_3^--N and NH_4^+-N, which is considered to be the dominant pathway of soil N loss (Sebilo et al., 2013). It has been reported that NO_3^--N is much more easily absorbed by roots (Malhi et al., 1988; Kronzucker et al., 1997), so NO_3^--N was set as having a higher priority of being taken up by plant roots in each soil layer using the following Eq (2) and Eq (3):

$$demand\_NO_{3\,i}^{-} = COE_{NO3} \cdot layer\_demand_i \cdot \frac{NO_{3\,i}^{-}}{(NO_{3\,i}^{-} + NH_{4\,i}^{+})}, \quad (2)$$

$$demand\_NH_{4\,i}^{+} = layer\_demand_i - demand\_NO_{3\,i}^{-}. \quad (3)$$

Here, $demand\_NO_{3\,i}^{-}$ and $demand\_NH_{4\,i}^{+}$ are the plants' NO_3^- and NH_4^+ requirements from soil layer i; and $layer\_demand_i$ is the total plant N uptake requirement from soil layer i. COE_{NO3} is the coefficient of nitrate demand, which was set to 4.0 according to the model test. The comparison between the tendency of the modeled soil nitrate content and the detected soil nitrate concentration proved the effectiveness of the model design (Fig. S1).

Harvest: Harvest practices significantly reduce the soil C and N inputs for cropland compared with natural soil. We systematically removed all of the litterfall from the cropland ecosystem at the end of the growing seasons to modify the harvest.

2.2.2 N Input

The input N flows of agricultural soil include N fertilizer, biological N fixation, atmospheric deposition, and returned straw (Liu et al., 2010). We integrated chemical N fertilization, manure application, and returned straw processes into the original model.

Returned residues: Returned residues are a significant C and N source for cropland soil and a recommended practice for improving N use efficiency. It has been reported that more than half of the N in crops (all of which is taken up from the soil) is removed from the ecosystem, and only 20% of the crop's N is returned to the soil N pools as returned residues globally (Liu et al., 2010). Therefore, in our model, we returned 20% of the harvested plants to the cropland soil in order to modify the returning residue practices.

Chemical N fertilizer: Chemical N fertilizers were directly added to the NO_3^- and NH_4^+ pools of the top layer of soil in the original model.

Manure N fertilizer: The manure-sourced N entered the different inorganic N and organic N pools separately. The organic portion of the manure was added to up to 3 soil organic matter (hereafter SOM) pools (the non-protected, protected, and passive organic carbon pools) separately for further decomposition (Zhang et al., 2017b).

$$ManureNH_4^{+} = R_{NH4} \cdot Manure_N. \quad (4)$$

$$ManureNO_3^{-} = R_{NO3} \cdot Manure_N. \quad (5)$$

https://doi.org/10.5194/gmd-2021-23
Preprint. Discussion started: 20 April 2021


Geoscientific Model Development Discussions

$$ManureC_{SOM} = proportion_{SOM} \cdot C{:}N_{SOM} \cdot Manure_N. \quad (6)$$

Here, $ManureNH_4^+$ and $ManureNO_3^-$ are manure-sourced NH_4^+-N and NO_3^--N, respectively, which are calculated using the ratio of ammonia and nitrate (i.e., R_{NH4} and R_{NO3}) to total manure N. $ManureC_{SOM}$ is the amount of manure that entered the different SOM pools; $proportion_{SOM}$ is the proportion of manure N added to the different SOM pools; and $C{:}N_{SOM}$ is the C:N ratio of a particular SOM pool.

2.2.3 Irrigation and tillage

Some agricultural practices do not directly alter the N flow in cropland soil, instead they affect N_2O by regulating the soil's physical properties.

Irrigation: The irrigation process used in this study adopted the idea of precipitation events from the DNDC (Li et al., 2000) and Agricultural Production Systems sIMulator (APSIM) (Thorburn et al., 2010). Similar to rainfall, irrigation provides extra water to the surface of the cropland soil, promoting the water-filled pore space (hereafter WFPS), thus stimulating the growth of the anaerobic balloon. Nevertheless, it simultaneously induces leaching and runoff processes. In the current model, only the flood irrigation method was included.

Tillage: Tillage redistributes the soil profile and increases the availability of oxygen in each soil layer at the same time. We averaged each of the C and N pools of the top 3 soil layers (as a global conventional tillage depth) after every tillage event. Because of more exposure to oxygen, the anaerobic conditions and diffusion pattern also vary with the different soil moisture conditions, properties, and vegetation types (Rochette, 2008; van Kessel et al., 2013).

3. Data and methods

3.1 Model sensitivity analysis

We conducted initial sensitivity analysis experiments to obtain the most sensitive parameters before testing the model. According to previous N_2O modeling studies (Zhang et al., 2017b; Zhang et al., 2019), the coefficient of nitrification (hereafter COE_{NR}) is the key parameter driving the amount of emitted N_2O in natural ecosystems probably because of the limited NO_3^- input. In this study, considering the increased NO_3^- input from fertilizers in cropland soil, it is conceivable for denitrification to become the dominant N_2O source. Therefore, 13 major parameters, including COE_{NR} and parameters associated with denitrification (Table1), were compared in a site-specific manner. The sensitivity index (SI) in this study followed the method of Lenhart et al. (2002) using the following Eq(7):

$$SI = \frac{1}{n} \cdot \sum_{j=1}^{n} \left(\frac{(y_{2j} - y_{1j})/y_{0j}}{2 \cdot \Delta x / x_0}\right), \quad (7)$$

where n is the total number of months from 1961 to 2015 (because in our model, chemical fertilizer application started in 1961); j accounts for the number of months from 1961 to 2015 (because in our model, chemical fertilizers were used after 1961); y_{0j} represents the jth monthly N_2O emissions with an initial parameter x_0; and y_{2j} *and* y_{1j} are the N_2O emission

https://doi.org/10.5194/gmd-2021-23
Preprint. Discussion started: 20 April 2021


Geoscientific Model Development Discussions

values produced for $+\Delta x$ and $-\Delta x$, respectively. Δx was set as 20% of x_0.

3.2 Model input data, calibration, and validation

3.2.1 Studied sites

We compiled measured N_2O emission data from croplands in published studies and the locations of the selected sites were distributed across most of the dominant terrestrial area. Most of the major crop types (maize, wheat, corn, sugarcane, vegetables, and cotton) were represented. The detailed site information is listed in Table 2, including the geographic location (latitude, longitude, and specific site), experimental period, dominate crop type, average N dose, soil properties (soil organic carbon, hereafter SOC, soil pH, soil texture), average daily N_2O emissions during the experimental period, and other agricultural practice information. Table S2 provides similar information on the dataset used for the validation.

3.2.2 Input data

All of the input information for the model simulation of the selected sites described above was directly obtained from the following datasets or was obtained from papers (see details below). These data were transformed into a spatial resolution of 0.5°×0.5° latitude/longitude using the ArcMap software (version 10.2) before the simulation.

Daily climate data: We obtained daily climate data from the CRUNCEP dataset (https://www.earthsystemgrid.org/dataset/ucar.cgd.ccsm4.CRUNCEP.v4.TPHWL6Hrly.html), including the minimum, average, and maximum temperature, precipitation, specific humidity, air pressure, and wind speed, which were used to drive the model.

N fertilization data: The historical chemical fertilizer (1961–2010) and manure (1860–2014) application data for croplands were derived from the datasets produced by Nishina et al. (2017) and Zhang et al. (2017), respectively.

The synthetic N fertilization dataset is mostly based on country-specific information from the Food and Agriculture Organization statistics (FAOSTAT) after filling data gaps (Nishina et al., 2017). Notably, the dataset provided application date and monthly input N fertilizer differentiated into NH_4^+ and NO_3^- considering the seasonal crop calendars for the dominant crops in each grid (Sacks et al., 2010). The synthetic N application rates in 2011–2015 were assumed to be the same as that for 2010. In addition, if the amount and type of N fertilizer from Nishina et al. (2017) failed to match the site information obtained from the literature, we utilized the site-specific amount of fertilizer application according to the published paper and the NH_4^+-N/ NO_3^--N ratio provided by Nishina et al. (2017).

The manure N dataset (Zhang et al., 2017a) included the annual manure production and annual application, which were reconstructed using the dataset from the Global Livestock Impact Mapping System (GLIMS) in conjunction with country-specific annual livestock populations and the gridded cropland distribution map for 1860–2014 obtained from HYDE 3.2 (Goldewijk et al., 2017). The manure N production and application rates in 2015 were assumed to be the same as those in 2014.

https://doi.org/10.5194/gmd-2021-23
Preprint. Discussion started: 20 April 2021


Geoscientific Model Development Discussions

N deposition data: We extracted the annual N deposition data based on the global maps of atmospheric nitrogen deposition (1993) (Dentener, 2006; http://daac.ornl.gov/cgi-bin/dsviewer.pl?ds_id5830) supported by a three-dimensional global chemistry transport model (TM3) (Lelieveld and Dentener, 2000), which used N emission estimates (van Aardenne et al., 2001) and projection scenario data (Houghton, 1996; Nakicenovic et al. 2000).

Vegetation: For the model initialization, we generated vegetation cover data by overlaying the Global Land Cover Map for 2009 (GlobCover2009) based on Medium Resolution Imaging Spectrometer (MERIS) remote sensing data (http://due.esrin.esa.int/page_globcover.php) with the ecoregions framework from the World Wildlife Fund (WWF). Then, we generated a new category of global vegetation cover types that fitted the plant functional type of the model and relied on these land cover data. The annual cropland area from 1860 to 2015 was acquired from the History Database of the Global Environment, version 3.2 (HYDE 3.2), which has reconstructed time-dependent land use using historical population and allocation algorithms with weighting maps (Goldewijk et al., 2017). Cropland can be classified into rain-fed and irrigated land, both of which were further divided into rice, generic C_3 crops (except rice, e.g., wheat), and generic C_4 crops (e.g., maize) based on the global crop distribution maps (Monfreda et al., 2008).

Soil data: The global soil properties (soil texture and soil pH) and classification were obtained from the Food and Agriculture Organization/United Nations Educational, Scientific and Cultural Organization (FAO/UNESCO) Soil Map of the World (http://www.fao.org/geonetmork/srv/en/metadata.show?id514116) and the dataset provided by Batjes (2006), respectively. The soil C and C:N ratio data used for the model initialization were generated from a global soil dataset (IGBP-DIS; 2000).

Topographic data: We used a global digital elevation model (DEM) with an approximate spatial resolution of 1 km (GTOPO30) for the topography input (http://www.temis.nl/data/gtopo30.html).

Atmospheric CO_2 concentration data: The monthly atmospheric CO_2 concentration data for the simulation period from 1860 to 2015 was obtained from the National Oceanic and Atmospheric Administration (NOAA) GLOBALVIEW-CO_2 dataset derived from atmospheric and ice core measurements (www.esrl.noaa.gov).

3.2.3 Model Calibration and Validation

The daily N_2O flux data for 39 sites were used for the model calibration, and the mean daily emission data for 69 other sites were used for the model validation. We estimated the model parameters, soil properties, and vegetation information from our input datasets, and used the agricultural practice's information obtained from the corresponding literature (Table 2), e.g., the amount of N input, to set up the model.

Before the model simulation and analysis, a spin-up period of about 300 years was conducted until the soil biogeochemical cycles and the compositions of the different C and N pools remained in equilibrium under stationary climate

https://doi.org/10.5194/gmd-2021-23
Preprint. Discussion started: 20 April 2021


Geoscientific Model Development Discussions

conditions, which was the multiyear mean climate data.

For the model calibration, we used the daily climate data for each site to drive the model along with other site-specific input information. The simulation started on January 1st, 1901, and ended on December 31st, 2015, with a daily time step. By comparing the output N_2O flux data with the observed data, we adjusted the most sensitive parameter of the N_2O emissions based on the sensitivity analysis in order to fit the best model performance via trial and error and statistical model performance indicators. The index of agreement (*D*), the root mean square error (*RMSE*), and the coefficient of determination (R^2) were used to evaluate our model's performance, and the D-value and *RMSE* were calculated as follows:

$$D = 1 - \frac{\sum_{i=1}^{n}(S_i - O_i)^2}{\sum_{i=1}^{n}(|S_i - \overline{O}| + |O_i - \overline{O}|)^2}, \quad (8)$$

$$RMSE = \sqrt{\frac{\sum_{i=1}^{n}(S_i - O_i)^2}{n}}. \quad (9)$$

Here, S_i is the ith simulated result corresponding to the number of observations; O_i is the ith observed value; and $\overline{O}$ is the mean of the observed values during the experimental period. D varies between 0 and 1, and is excessively sensitive to extreme values (Willmott, 1981). The model performance was considered to be perfect and unmeaningful when the D value was set to 1 and 0, respectively. The *RMSE* is the key value representing the difference between the simulated and observed values, and is significantly affected by the data units.

Based on the calibration results and the fitting of the most sensitive parameter for the different sites, we used the continental mean parameter for the model validation.

4. Results

4.1 Sensitivity analysis

The mean sensitivity index (*SI*) varied from -0.53 (EFF_{NO2}) to 1.37 (COE_{dNO3}) for the selected 13 parameters (Fig. 2). All of the parameters had a nonunique effect on the N_2O emissions of the different sites. COE_{dNO3}, COE_{NR}, MUE_{NO3}, M_{NO3}, EFF_{N2O}, COE_{dNO2}, and COE_{dNO} mostly had positive effects, while the remaining parameters either had negative effects (e.g., MUE_{N2O} and EFF_{NO2}) or had no evident impact (e.g., AMAX) on the N_2O fluxes. The coefficient of the NO_3^- consumption rate (COE_{dNO3}) was the most sensitive parameter in the current TRIPLEX-GHG model. The *SI* ranged from -0.61 to 5.39 (with a mean of 1.37) for the current model input information. We also noticed that the *SIs* of the selected parameters were not consistent with the different input information, especially for the variations in the amount of N fertilizer applied. The COE_{dNO3} slightly increased initially and then decreased as the N dose increased; and as the most sensitive parameter, it retained a large *SI* value (Fig. S2).

Overall, to simplify the parameter fitting processes and to evaluate the model's performance, we selected COE_{dNO3} as the fitting parameter, while we set the other parameters to their original constant values as the default (Table 1).

4.2 Model calibration

https://doi.org/10.5194/gmd-2021-23
Preprint. Discussion started: 20 April 2021


Geoscientific Model Development Discussions

The calibration sites were categorized into six main regions according to their geographical distribution, including North America (NA), Asia (AS), Europe (EU), Australia (AU), South America (SA), and Africa (AF). Generally speaking, the model's performance was reasonably good in terms of the comparison of the site observations with the modeled results (Table 3).

4.2.1 North American sites

The data collected for the North American cropland sites were located in the US and Canada and represented the dominant commercial crop species such as corn, wheat, barley, and tomatoes. Most of the measurements were collected over more than two years. For the sites located in the great lakes region (NA-1 and NA-2), the modeled seasonal patterns of the N_2O emission were generally consistent with the measured data (Figs. 3a–b), but the estimated pulses had longer durations than the observations (the model could not capture the detailed variations in the detected N_2O fluxes), which resulted in low agreement indices (D=0.65, D=0.56). For the studies carried out in the eastern Atlantic coastal region, the annual variation in the field data from site NA-3 was reproduced well by the model (Fig. 3c), except for some underestimated peak values, which slightly reduced the level of the model evaluation indices (D=0.69, $RMSE$ = 3.6, R = 0.57). Furthermore, the modeled simulation results were well matched for the scattered detected values of sites NA-4 and NA-5 (Figs. 3d–3e), with model agreement indices of 0.81. The model's results were also strongly correlated with the other collected observation data in the central (NA-6), southern (NA-7) USA, and western coastal regions of the continent (NA-8, NA-9). The model performed well for the long-term fertilized corn sites in Colorado (Fig. 3f; D = 0.84, $RMSE$ = 0.90, R = 0.73). Nevertheless, the model's results showed relatively low evaluation indices (D = 0.59, $RMSE$ = 4.09, R = 0.40) due to underestimating the length of the intensive emission period in July 2014 at site NA-7 (Fig. 3g). Moreover, its failure to capture the emission peaks in 2011/10 and 2012/10 for the California tomato site slightly jeopardized the model's performance (Fig. 3h; D = 0.61, $RMSE$ = 0.87, R = 0.48). As for site NA-9, the general trends of the modeled N_2O flux results were consistent with the observation data (Fig. 3i; D = 0.75, $RMSE$ = 0.92, R = 0.84).

4.2.2 Asia

Ten upland agricultural sites were selected in Asia (Table 2 and Fig. 4), including one in central India (AS-1), one in Japan (AS-7), one in the Aral Sea Basin, Uzbekistan (AS-10), and several in China. All of the selected sites were characterized by long-term cultivation histories and intense agricultural activities.

In general, the model captured the main variations in the observations and agreed well with all of the daily observations for most of the sites, except for conventional cropland sites AS-1 and AS-2. The observed N_2O variations in site AS-1 were overestimated (2009/7, 2010/1, and 2010/4) and underestimated (2008/7 and 2010/4) compared with the simulated results, leading to an agreement index of 0.69 (Fig. 4a). According to the observed N_2O emission rates for site AS-2 reported by Guo et al. (2013), certain points were being recorded as negative values without apparent regularity in the time series, while the

https://doi.org/10.5194/gmd-2021-23
Preprint. Discussion started: 20 April 2021


Geoscientific Model Development Discussions

model was less robust in terms of capturing the occurrence of N_2O uptake, resulting in a low index of agreement (Fig. 4b, D = 0.50). In addition, the simulation exhibited reasonable N_2O flux variation patterns, especially the occurrence of emission pulses induced by fertilization, comparable to those described by Zhou et al. (2019) (Fig. 4c) and Zhang et al. (2016) (Fig. 4d), while the inaccurately estimated peak values suppressed the evaluation of the model's performance (AS-3, D = 0.67; AS-4, D = 0.64).

For the other selected sites in Asia, the model results for sites AS-5, AS-6, AS-7, and AS-8 showed that simulated N_2O fluxes agreed well with the observed fluxes under different agricultural practices, with model agreement indices of 0.86, 0.81, 0.78, and 0.76, respectively (Figs. 4e–h). Scattered observation points in a peanut site located in central-subtropical China were also simulated by our model and the result showed a similar general pattern of N_2O flux with acceptable model performance indices (Fig. 4i; D = 0.65, R = 0.49, $RMSE$ = 0.31). For the long-term wheat cultivation site in Uzbekistan, characterized by extremely high emission rates (>50 mg N m^{-2} day^{-1}), the simulated N_2O emission rate matched the observations well, except for one overestimated emission pulse in 2005/7 (Fig. 4j), which resulted in model performance indicators of D = 0.74, R = 0.60, and $RMSE$ = 6.03.

4.2.3 Europe

Most of the wide-spread crop types were included in the calibration of the model simulation of the European cropland sites, which were located in the mid-high latitude region. The simulated trends and magnitudes of N_2O were generally consistent with the measured data for most of the sites, but some of them had relatively low agreement indices. Based on the studies of Kavdir et al. (2008) and Senapati et al. (2016), the frequent failure of capturing the major emission pulses, such as the one induced by fertilizer input in 2003/1 for EU-1 (Fig. 5a) and the one that occurred in 2013/6 for EU-2 (Fig. 5b), accounted for the low agreement indices (D = 0.51 and 0.53, respectively). Moreover, the low evaluation indices of site EU-3 (D = 0.52) are attributed to the estimation gap between the simulated and observed peak values and the duration time (e.g., overestimated emission peak in 2004/7) as well as the underestimation of the background emissions (Fig. 5c). The study carried out by Hall et al. (2010) reported extremely high N_2O emission rates due to the application of large amounts of manure. The model had a low agreement index because it underestimated the major peaks and the duration (Fig. 5d; D = 0.61).

Additionally, the model simulation also revealed good agreement with the measured N_2O emission data for the other European sites. For the site observations provided by Sosulski et al. (2015) and Baggs et al. (2003), the modeled emission rates matched the observed scatter points reasonably well (Figs. 5e–f), with good agreement indices (D = 0.75 and 0.79, respectively). As for sites EU-7 and EU-8, the modeled daily N_2O emission rates reflected the general trends of the N_2O emissions in response to fertilization and irrigation practices well. However, the modeled results still mis-captured the minor emission pulses in 2009/1 at site EU-7 (Fig. 5f; D = 0.77, $RMSE$ = 1.46, R = 0.66) and in 2007/8 at site EU-8 (Fig. 5g; D = 0.87, $RMSE$ = 0.23, R = 0.75). The model is sensitive to fertilizer application and produced well-simulated results comparing with the measured data collected in Madrid (Fig. 5h; D = 0.91, $RMSE$ = 1.36, R = 0.88).

https://doi.org/10.5194/gmd-2021-23
Preprint. Discussion started: 20 April 2021


Geoscientific Model Development Discussions

4.2.4 Oceanic

Almost all of the cropland N_2O studies carried out in Australia were located in the eastern coastal region, and only one rainfed continuous wheat site in western Australia was used in the model calibration. The low model evaluation indices of site AU-1 (D = 0.47, $RMSE$ = 0.12, R = 0.25) are probably associated with the failure to capture the emission peaks in 2006/1, 2007/4, and 2010/3 (Fig. 6a). For the other sites in eastern Australia, the general seasonal patterns of the simulated N_2O emission were consistent with the observations. The model performed reasonably well for manure dominated site AU-2, and the overestimated peak value was responsible for the low agreement index (Fig. 6b; D = 0.69). A lychee (*Litchi chinensis*) orchard site with a high sampling frequency was included, so we used the daily mean flux for the comparison. Notably, the PFT was considered to be subtropical forest for this site, and the model performed well (Fig. 6c; D = 0.80, R = 0.75) even though there was an obvious mis-capture of the emission peak in 2008/6. It should be noted that sugarcane was planted at site AU-5. Because the C properties of sugarcane differ significantly from those of grain crops (e.g. wheat), the PFT was set as shrub during the calibration. The modeled results of the sugarcane-based crop systems agreed well with the measured data (Fig. 6e; D = 0.73, $RMSE$ = 0.65, R = 0.55).

4.2.5 South America & Africa

Unfortunately, there are insufficient observations of cropland N_2O emissions conducted in the agriculturally dominated regions of South America and Africa (Fig. 7 and Table 2). Typical agricultural ecosystems in these regions (sugarcane, wheat) were selected for the model calibration. Compared with the results of the two sites with short experimental periods in Africa (Figs. 7a–b), the simulated seasonal N_2O variation agreed reasonably well with the one year of observations as is indicated by model performance indices (AF-1: D = 0.92, $RMSE$ = 0.22, R = 0.94; and AF-2: D = 0.87, $RMSE$ = 0.65, R = 0.93).

In South Africa, both cereal and economic crop sites were included. The model results were in good agreement with the measured N_2O emission rates reported by Passianoto et al. (2003) even though the number of points were limited (Fig. 7c; D = 0.93, $RMSE$ = 0.70, R = 0.90). Moreover, the modeled results also illustrated that the N_2O variation patterns for the model simulations and the observations are good agreement for the maize-wheat site SA-2, but the model mis-captured minor pulses, slightly reducing the evaluation index (Fig. 7d; D = 0.81, $RMSE$ = 4.19, R = 0.67). For the sugarcane site SA-3, the simulated results were generally well correlated with the measured N_2O fluxes, which are highly regulated by the agricultural practices; however, the model failed to capture the consistent relatively high-level emission rates after fertilizer application (Fig. 7e; D = 0.74, $RMSE$ = 1.25, R = 0.65).

In summary, according to the calibration results, the trends and magnitudes of the simulated N_2O flux were generally consistent with the measured field data.

4.3 Model validation

The model validation (Fig. 8) involved comparing the simulated and measured daily mean of the N_2O emissions for all

https://doi.org/10.5194/gmd-2021-23
Preprint. Discussion started: 20 April 2021

of the validated sites, and the results are also presented in Table S2. During the validation, the simulated daily mean emission rates during the experimental periods ranged from 0.048 to 5.21 mg N m^{-2} day^{-1}, and most of the values were less than 1 mg N m^{-2} day^{-1}. The regression result was close to the 1:1 line, indicating that the modeled results are quite consistent with the observed N_2O emissions (R^2 = 0.86, p<0.001). However, the modeled results tend to slightly underestimate the N_2O flux for the low observation values (<1 mgN m^{-2} day^{-1}) and to overestimate for large observed N_2O flux values (>1 mgN m^{-2} day^{-1}). The model validation results further confirm that our model is capable of simulating the impacts of both climate and agricultural practices on N_2O emissions across global cropland ecosystems.

5. Discussion

It is important to calibrate the process-based model using reasonable parameters in order to simulate complex biogeochemical processes better. Adjusting the most sensitive parameter is an efficient method of improving the model performance and has been widely used in model development and parameterization (Wang and Chen 2012; Zhang et al., 2017b; Zhu et al., 2014). As was stated in a previous study, Zhang et al. (2017) tested 23 parameters and found that the COE_{NR}, the coefficient of the nitrification rate, controlled the N_2O emission process. Meanwhile, our sensitivity analysis results revealed that the coefficient of the nitrate consumption rate, COE_{dNO3}, had the highest sensitivity level for the updated version of the TRIPLEX-GHG model. Such a divergence is probably due to the increased N input, especially NO_3^-, in cropland ecosystems compared with natural grasslands and forests. Denitrification strongly contributes to N_2O production in agricultural ecosystems, which requires NO_3^- as a substrate (Wang et al., 2018a). Since it is controlled by this parameter, the NO_3^- consumption (from NO_3^- to NO_2^-) dominates the denitrification rate and thus the N_2O production rate of N fertilized soil. Globally, the COE_{dNO3} exhibited a large range of variation during the parameterization, which can partly be reconciled by the calibration method and the varying amounts of mineral N input. Because the NO_3^- consumption rate for denitrification is difficult to measure directly, the limited field information strongly discourages the systematic adjustment of the $COE_{dNO3,}$ and thus, the potential uncertainty of the parameter affected the model's performance.

Generally, the TRIPLEX-GHG model reproduces the N_2O emissions well for a daily time step and various cropland ecosystems (e.g., wheat, maize, sugarcane, and cotton) on a global scale. The dominant characteristic of cropland N_2O emission is the peaks associated with fertilization events, most of which were well simulated by our model and contributed to overall reasonable evaluation indices. Such advantages were derived from three features of our model. First, both the soil oxygen conditions and the soil water conditions were considered in the TRIPLEX-GHG model, i.e., represented by the size of the anaerobic balloon and the water-filled pore space, respectively. Previous studies have highlighted that the soil O_2 status is the proximal, direct, and most decisive environmental trigger of N_2O production (Song et al., 2019; Zhu et al., 2013; Khalil et al., 2004). However, the majority of process-based models only integrated the WFPS into the nitrification and denitrification

https://doi.org/10.5194/gmd-2021-23
Preprint. Discussion started: 20 April 2021


Geoscientific Model Development Discussions

processes (e.g., Tian et al., 2010; Ito et al., 2018). It was reported that although the WFPS is a critical element containing information about the soil water and gaseous status, it still requires combination with other soil structural parameters in order to better predict the soil O_2 concentration, microbial respiration, and subsequent gas diffusion (Farquharson and Baldock, 2008; Song et al., 2019; Hall et al., 2013; Rabot et al., 2015). Second, a detailed description of the manure also contributed to the improved model performance because manure is a predominant soil organic carbon (SOC) source for croplands, which is not considered by empirical models and several of the process-based models (e.g., DAYCENT, VISIT). The SOC serves as a key energy and carbon source for microbial growth, nitrification, and denitrification (Snyder et al., 2009; Butterbach-Bahl et al., 2013). Field observations have shown that the application of manure either promotes or reduces N_2O emissions probably because the added organic C compounds support microbial growth, but the increased SOC stimulates complete denitrification with the further reduction of N_2O to N_2 (Zhou et al., 2017; Meijide et al., 2007). Therefore, in this study, the manure sourced C was recalculated using the manure N and C:N ratio, which significantly enhanced the simulation of the SOC. Last but not least, the TRIPLEX-GHG model included a reasonable microbial growth and death description, which strongly improved the accurate modeling of the nitrification process because the soil microbial conditions are one of the primary determinants of the soil nitrification rate at a global scale (Li et al., 2020).

However, there are still major discrepancies between the modeled and measured N_2O fluxes, including underestimated peak values, failure to capture emission peaks, and underestimated background emissions. First, although the timing of the simulated major emission pluses was well simulated, the peak values of the emitted N_2O fluxes were underestimated. The incomplete description of the processes involving the interaction between the soil pH and the external mineral N input is probably responsible for this phenomenon. The soil pH is one of the most important drivers of N_2O production. Acidic soils are more sensitive to N input than alkaline soils, which probably enhances N_2O production in croplands (Wang et al., 2018b; Morkved et al., 2007). Studies have shown that the pH values of agricultural soil tend to be significantly reduced by N deposition and N-fertilization at the global scale (Tian and Niu, 2015; Godsey et al., 2007; Guo et al., 2010). However, because the soil buffer capacity is difficult to quantify (Baron et al., 2014; Zhang et al., 2017b), the soil pH in our model was input information with a consistent pH value for each grid, and we neglected the effect of N input on soil pH such as the hydrolysis of urea (Tian and Niu, 2015; Wang et al., 2018b).

Next, the simulated results occasionally failed to capture several peaks in the observed N_2O emission values. The mis-capture or underestimation of these peak values became evident in early spring when freeze–thaw events occurred (Figs. 4h and 5g). Freeze–thaw induced N_2O emission pules constitute a major component of the annual total N_2O emission at high latitudes (Wagner-Riddle et al., 2017; Kim et al., 2012) because increased soil temperature significantly promotes both soil physical mechanisms and microbial metabolism (Wolf et al., 2010; Wagner-Riddle et al., 2017). The former helps release the trace gases accumulated and trapped within the ice layer, and it simultaneously stimulates the formation of anaerobic conditions

https://doi.org/10.5194/gmd-2021-23
Preprint. Discussion started: 20 April 2021


Geoscientific Model Development Discussions

(Teepe et al., 2004; Groffman et al., 2006). The latter triggers microbial driven nitrification and denitrification processes (Sharma et al., 2006). The limited description of those processes, especially the simple empirical parameters and algorithms we used for modeling snow-melting hydrology and nutrient release, are the primary error sources (Zhang et al., 2017b).

Furthermore, as for the underestimated background emissions, it is still a significant challenge for the process-based model to accurately quantify background N_2O emissions due to the following possible reasons. First, our simulations used general crop classification (C_3, C_4, and rice) instead of detailed crop rotation information with different physiological parameters (Ito et al., 2018; Monfreda et al., 2008; Saikawa et al., 2013). Field observations have revealed that different crop types or species have diverse impacts on the N_2O fluxes of cropland (Rochette et al., 2018; Philibert et al., 2013; Petersen et al., 2006; Gelfand et al., 2016). For instance, legume species (e.g., soybean) have a stronger N fixation ability, which contributes considerably to the N pools in cropland soil (Liu et al., 2010), and they effectively promote background N_2O emission even without N fertilization compared with other cereal crops (Lenka et al., 2017; Sanchez and Minamisawa, 2019; Yang and Cai, 2005). Second, in addition to climate conditions, the background emission rates from agricultural soils are also associated with the amounts of residual N added in preceding years (Aliyu et al., 2018; Gu et al., 2009), and thus, the types of residuals also have varying effects on the N_2O emissions (Shan and Yan, 2013). Our model used the global mean ratio of the returned residual N to the total plant biomass N for the simulation (Liu et al., 2010; Meng et al., 2005; Zhou et al., 2017) because these agricultural practices are controlled by the individual farmers and vary greatly at the local and subregional scales, without clear global distribution patterns such as those for soil and climate (Wang et al., 2018b). Third, the uncertainties in the site history are also responsible for the inaccuracy of the modeled background emissions because the site history has a tremendous effect on the soil properties, especially the SOC content (Gelfand et al., 2016). Previous studies have demonstrated that agricultural practices, such as returning residues to the soil, tillage management, and fertilizer application, are important drivers of the SOC (Liu et al., 2014; Jiang et al., 2018; Zhou et al., 2017), but their effects vary with the intensity of the practices and the climatic conditions (Ogle et al., 2019; Snyder et al., 2009; van Kessel et al., 2013; Liu et al., 2014; Gattinger et al., 2012). Unfortunately, only a few published papers have provided detailed historical land use and agricultural practice information, which is a barrier to the accurate estimation of the local SOC and thus N_2O emissions.

Last but not least, the other reasons for the discrepancies between the modeled results and the observations may be the uncertainties in the field measurements and the driving data. For one, the lower sampling frequency of the fieldwork and the short-lived N_2O emission pluses are particularly difficult to captured with traditional manual chambers, especially after base fertilizer application in the fallow season (Lammirato et al., 2018; Lognoul et al., 2019). Moreover, the model's accuracy also relies on good quality data. A 0.5°×0.5° global scale daily climate input dataset was used for the model calibration and validation, but it is unlikely that every site was provided with detailed meteorological information due to the relatively coarse spatial resolution. The local climate may differ significantly from that of the grid input information (Wania et al., 2010).

https://doi.org/10.5194/gmd-2021-23
Preprint. Discussion started: 20 April 2021


Geoscientific Model Development Discussions

Specifically, the precipitation information is less accurate compared with the other climate data, which could significantly jeopardize the model's performance since the anaerobic balloon is a precipitation-induced process (Zhang et al., 2017b). Furthermore, the soil properties are also difficult to be precisely replicate at the site level using a global soil dataset. Because the soil texture served as a significant driver for the N_2O emissions (Philibert et al., 2013; Gu et al., 2013), the mismatch of soil information is also a major cause of the disagreement between the model simulations and observations.

In response to the uncertainties described above, further modeling is suggested to improve the detail of the descriptions of the key processes, and better quality datasets need to be collected.

First, it is recommended that more detailed soil microbial activities be considered in order to better model the features of the N_2O emissions (Li et al., 2020). The nitrifier-denitrification process may account for up to 100% of the N_2O emissions from NH_4^+ in soils (Wrage et al., 2001; Wrage-Moennig et al., 2018), especially for N_2O uptake, the occurrence of which has been widely observed in peatlands, boreal forests, (Saikawa et al., 2013) and occasionally in cropland ecosystems (e.g., Fig. 4b). In addition, ammonia oxidation has been found to be a significant process for the development of N_2O compared to classical denitrification in extremely low-oxygen concentration soils (Zhu et al., 2013).

Next, in this study, only general PFTs were used for croplands without specifying crop types, for which the nutrient requirements, maximum productivities, C:N ratios of different organs, and biomass allocation patterns differ significantly from each other (Li et al., 2000; Shan and Yan, 2013), which significantly affects the N dynamics of cropland soils.

Furthermore, various agricultural management practices were not included in the current model. For example, different techniques of tillage (e.g. conventional tillage, minimum tillage, tillage with different instruments), irrigation (e.g., flood irrigation and drip irrigation), and fertilizer placement (e.g., top dressing and injection) can have diverse impacts on N_2O emissions (Maris et al., 2015; Rochette, 2008). For instance, drip irrigation effectively promotes WFPS without surface runoff, which induces significant N_2O flux (Sanchez-Martin et al., 2008). Considering the advantages of field studies, model performances can be effectively improved at the site level.

6. Conclusions

Our study represents a successful attempt to fully integrate general agricultural activities into the current TRIPLEX-GHG framework for simulating global N_2O emissions across cropland ecosystems. In this study, the COE_{dNO3}, which controls the NO_3^- consumption rate of the denitrification process, was found to be the most sensitive parameter. The key parameter was calibrated using measured data for 39 global cropland sites, and we found that the improved TRIPLEX-GHG model was capable of simulating the dynamics and magnitudes of N_2O emissions from croplands at a daily time step, especially the emitted peaks associated with fertilizer application. The model validation results further confirm that the modeled N_2O emissions were highly correlated with the observed data. However, the model was unable to capture several detailed emission

https://doi.org/10.5194/gmd-2021-23
Preprint. Discussion started: 20 April 2021

characteristics, which jeopardized the model's performance. Further development of the TRIPLEX-GHG model could contribute to sustainable agricultural development, scientific modeling, and a better quantification of the global greenhouse gas budget under global change.

Code and Data availability The source code and configuration for the current version of the TRIPLEX-GHG model employed for the simulations is available at https://doi.org/10.5281/zenodo.4679490. All the model input datasets can be obtained from the cited publications and websites. Model input information for calibration and validation were derived from corresponding papers. Notably, the model output dataset can be required by contacting the first author.

Author contribution Changhui Peng and Qiuan Zhu designed the study. Hanxiong and Kerou developed the model code and performed all the simulations and model tests. Hanxiong prepared the manuscript with contributions from all co-authors.

Competing interests The authors declare that they have no conflict of interest.

Acknowledgements This study was funded by the Natural Sciences and Engineering Research Council of Canada Discovery Grant and the National Key R&D Program of China (2016YFC0500203). We thank LetPub (www.letpub.com) for its linguistic assistance during the preparation of this manuscript.

https://doi.org/10.5194/gmd-2021-23
Preprint. Discussion started: 20 April 2021

Reference

Abalos, D., Sanz-Cobena, A., Garcia-Torres, L., van Groenigen, J. W., and Vallejo, A.: Role of maize stover incorporation on nitrogen oxide emissions in a non-irrigated Mediterranean barley field, Plant and Soil, 364, 357-371, 10.1007/s11104-012-1367-4, 2013.

Aita, C., Schirmann, J., Pujol, S. B., Giacomini, S. J., Rochette, P., Angers, D. A., Chantigny, M. H., Gonzatto, R., Giacomini, D. A., and Doneda, A.: Reducing nitrous oxide emissions from a maize-wheat sequence by decreasing soil nitrate concentration: effects of split application of pig slurry and dicyandiamide, European Journal of Soil Science, 66, 359-368, 10.1111/ejss.12181, 2015.

Aliyu, G., Sanz-Cobena, A., Mueller, C., Zaman, M., Luo, J., Liu, D., Yuan, J., Chen, Z., Niu, Y., Arowolo, A., and Ding, W.: A meta-analysis of soil background N2O emissions from croplands in China shows variation among climatic zones, Agriculture Ecosystems & Environment, 267, 63-73, 10.1016/j.agee.2018.08.003, 2018.

Alvaro-Fuentes, J., Luis Arrue, J., Bielsa, A., Cantero-Martinez, C., Plaza-Bonilla, D., and Paustian, K.: Simulating climate change and land use effects on soil nitrous oxide emissions in Mediterranean conditions using the Daycent model, Agriculture Ecosystems & Environment, 238, 78-88, 10.1016/j.agee.2016.07.017, 2017.

Baggs, E. M., Stevenson, M., Pihlatie, M., Regar, A., Cook, H., and Cadisch, G.: Nitrous oxide emissions following application of residues and fertiliser under zero and conventional tillage, Plant and Soil, 254, 361-370, 10.1023/a:1025593121839, 2003.

Berdanier, A. B., and Conant, R. T.: Regionally differentiated estimates of cropland N2O emissions reduce uncertainty in global calculations, Global Change Biol., 18, 928-935, 10.1111/j.1365-2486.2011.02554.x, 2012.

Betlach, M. R., and Tiedje, J. M.: Kinetic explanation for accumulation of nitrite, nitric oxide, and nitrous oxide during bacterial denitrification, Appl. Environ. Microbiol., 42, 1074-1084, 1981.

Botta, A., Viovy, N., Ciais, P., Friedlingstein, P., and Monfray, P.: A global prognostic scheme of leaf onset using satellite data, Global Change Biol., 6, 709-725, 10.1046/j.1365-2486.2000.00362.x, 2000.

Bouwman, A. F., Boumans, L. J. M., and Batjes, N. H.: Modeling global annual N2O and NO emissions from fertilized fields, Global Biogeochemical Cycles, 16, 10.1029/2001gb001812, 2002.

Buchkina, N. P., Balashov, E. V., Rizhiya, E. Y., and Smith, K. A.: Nitrous oxide emissions from a light-textured arable soil of North-Western Russia: effects of crops, fertilizers, manures and climate parameters, Nutrient Cycling in Agroecosystems, 87, 429-442, 10.1007/s10705-010-9349-5, 2010.

Burney, J. A., Davis, S. J., and Lobell, D. B.: Greenhouse gas mitigation by agricultural intensification, Proceedings of the National Academy of Sciences of the United States of America, 107, 12052-12057, 10.1073/pnas.0914216107, 2010.

https://doi.org/10.5194/gmd-2021-23
Preprint. Discussion started: 20 April 2021

Butterbach-Bahl, K., Baggs, E. M., Dannenmann, M., Kiese, R., and Zechmeister-Boltenstern, S.: Nitrous oxide emissions from soils: how well do we understand the processes and their controls?, Philosophical Transactions of the Royal Society B-Biological Sciences, 368, 10.1098/rstb.2013.0122, 2013.

Cai, Z., Wang, B., Xu, M., Zhang, H., Zhang, L., and Gao, S.: Nitrification and acidification from urea application in red soil (Ferralic Cambisol) after different long-term fertilization treatments, J. Soils Sed., 14, 1526-1536, 10.1007/s11368-014-0906-4, 2014.

Carlson, K. M., Gerber, J. S., Mueller, N. D., Herrero, M., MacDonald, G. K., Brauman, K. A., Havlik, P., O'Connell, C. S., Johnson, J. A., Saatchi, S., and West, P. C.: Greenhouse gas emissions intensity of global croplands, Nature Climate Change, 7, 63-+, 10.1038/nclimate3158, 2017.

Cavigelli, M. A., Del Grosso, S. J., Liebig, M. A., Snyder, C. S., Fixen, P. E., Venterea, R. T., Leytem, A. B., McLain, J. E., and Watts, D. B.: US agricultural nitrous oxide emissions: context, status, and trends, Front. Ecol. Environ., 10, 537-546, 10.1890/120054, 2012.

Chatskikh, D., Olesen, J. E., Berntsen, J., Regina, K., and Yamulki, S.: Simulation of effects of soils, climate and management on N(2)O emission from grasslands, Biogeochemistry, 76, 395-419, 10.1007/s10533-005-6996-8, 2005.

Chen, G., Kolb, L., Cavigelli, M. A., Weil, R. R., and Hooks, C. R. R.: Can conservation tillage reduce N2O emissions on cropland transitioning to organic vegetable production?, Science of the Total Environment, 618, 927-940, 10.1016/j.scitotenv.2017.08.296, 2018.

Cheng, K., Ogle, S. M., Parton, W. J., and Pan, G.: Simulating greenhouse gas mitigation potentials for Chinese Croplands using the DAYCENT ecosystem model, Global Change Biol., 20, 948-962, 10.1111/gcb.12368, 2014.

Cui, F., Yan, G., Zhou, Z., Zheng, X., and Deng, J.: Annual emissions of nitrous oxide and nitric oxide from a wheat-maize cropping system on a silt loam calcareous soil in the North China Plain, Soil Biology & Biochemistry, 48, 10-19, 10.1016/j.soilbio.2012.01.007, 2012.

Davidson, E. A.: The contribution of manure and fertilizer nitrogen to atmospheric nitrous oxide since 1860, Nature Geoscience, 2, 659-662, 10.1038/ngeo608, 2009.

Davidson, E. A., and Kanter, D.: Inventories and scenarios of nitrous oxide emissions, Environmental Research Letters, 9, 10.1088/1748-9326/9/10/105012, 2014.

Del Grosso, S. J., Parton, W. J., Mosier, A. R., Ojima, D. S., Kulmala, A. E., and Phongpan, S.: General model for N2O and N-2 gas emissions from soils due to dentrification, Global Biogeochemical Cycles, 14, 1045-1060, 10.1029/1999gb001225, 2000.

https://doi.org/10.5194/gmd-2021-23
Preprint. Discussion started: 20 April 2021

Del Grosso, S. J., Mosier, A. R., Parton, W. J., and Ojima, D. S.: DAYCENT model analysis of past and contemporary soil N(2)O and net greenhouse gas flux for major crops in the USA, Soil & Tillage Research, 83, 9-24, 10.1016/j.still.2005.02.007, 2005.

Del Grosso, S. J., Ojima, D. S., Parton, W. J., Stehfest, E., Heistermann, M., DeAngelo, B., and Rose, S.: Global scale DAYCENT model analysis of greenhouse gas emissions and mitigation strategies for cropped soils, Global Planet. Change, 67, 44-50, 10.1016/j.gloplacha.2008.12.006, 2009.

Denmead, O. T., Macdonald, B. C. T., Bryant, G., Naylor, T., Wilson, S., Griffith, D. W. T., Wang, W. J., Salter, B., White, I., and Moody, P. W.: Emissions of methane and nitrous oxide from Australian sugarcane soils, Agricultural and Forest Meteorology, 150, 748-756, 10.1016/j.agrformet.2009.06.018, 2010.

Drury, C. F., Yang, X. M., Reynolds, W. D., and McLaughlin, N. B.: Nitrous oxide and carbon dioxide emissions from monoculture and rotational cropping of corn, soybean and winter wheat, Canadian Journal of Soil Science, 88, 163-174, 10.4141/cjss06015, 2008.

Ehrhardt, F., Soussana, J.-F., Bellocchi, G., Grace, P., McAuliffe, R., Recous, S., Sandor, R., Smith, P., Snow, V., Migliorati, M. d. A., Basso, B., Bhatia, A., Brilli, L., Doltra, J., Dorich, C. D., Doro, L., Fitton, N., Giacomini, S. J., Grant, B., Harrison, M. T., Jones, S. K., Kirschbaum, M. U. F., Klumpp, K., Laville, P., Leonard, J., Liebig, M., Lieffering, M., Martin, R., Massad, R. S., Meier, E., Merbold, L., Moore, A. D., Myrgiotis, V., Newton, P., Pattey, E., Rolinski, S., Sharp, J., Smith, W. N., Wu, L., and Zhang, Q.: Assessing uncertainties in crop and pasture ensemble model simulations of productivity and N2O emissions, Global Change Biol., 24, E603-E616, 10.1111/gcb.13965, 2018.

Farquharson, R., and Baldock, J.: Concepts in modelling N2O emissions from land use, Plant Soil, 309, 147-167, 10.1007/s11104-007-9485-0, 2008.

Foley, J. A., Prentice, I. C., Ramankutty, N., Levis, S., Pollard, D., Sitch, S., and Haxeltine, A.: An integrated biosphere model of land surface processes, terrestrial carbon balance, and vegetation dynamics, Global Biogeochemical Cycles, 10, 603-628, 10.1029/96gb02692, 1996.

Forte, A., Fiorentino, N., Fagnano, M., and Fierro, A.: Mitigation impact of minimum tillage on CO2 and N2O emissions from a Mediterranean maize cropped soil under low-water input management, Soil & Tillage Research, 166, 167-178, 10.1016/j.still.2016.09.014, 2017.

Galbally, I. E., Meyer, M. C. P., Wang, Y.-P., Smith, C. J., and Weeks, I. A.: Nitrous oxide emissions from a legume pasture and the influences of liming and urine addition, Agriculture Ecosystems & Environment, 136, 262-272, 10.1016/j.agee.2009.10.013, 2010.

https://doi.org/10.5194/gmd-2021-23
Preprint. Discussion started: 20 April 2021

Gattinger, A., Muller, A., Haeni, M., Skinner, C., Fliessbach, A., Buchmann, N., Maeder, P., Stolze, M., Smith, P., Scialabba, N. E.-H., and Niggli, U.: Enhanced top soil carbon stocks under organic farming, Proceedings of the National Academy of Sciences of the United States of America, 109, 18226-18231, 10.1073/pnas.1209429109, 2012.

Gelfand, I., Shcherbak, I. I., Millar, N., Kravchenko, A. N., and Robertson, G. P.: Long-term nitrous oxide fluxes in annual and perennial agricultural and unmanaged ecosystems in the upper Midwest USA, Global Change Biol., 22, 3594-3607, 10.1111/gcb.13426, 2016.

Gerber, J. S., Carlson, K. M., Makowski, D., Mueller, N. D., de Cortazar-Atauri, I. G., Havlik, P., Herrero, M., Launay, M., O'Connell, C. S., Smith, P., and West, P. C.: Spatially explicit estimates of N2O emissions from croplands suggest climate mitigation opportunities from improved fertilizer management, Global Change Biol., 22, 3383-3394, 10.1111/gcb.13341, 2016.

Giltrap, D. L., Li, C., and Saggar, S.: DNDC: A process-based model of greenhouse gas fluxes from agricultural soils, Agriculture Ecosystems & Environment, 136, 292-300, 10.1016/j.agee.2009.06.014, 2010.

Godsey, C. B., Pierzynski, G. M., Mengel, D. B., and Lamond, R. E.: Changes in soil pH, organic carbon, and extractable aluminum from crop rotation and tillage, Soil Sci. Soc. Am. J., 71, 1038-1044, 10.2136/sssaj2006.0170, 2007.

Goldewijk, K. K., Beusen, A., Doelman, J., and Stehfest, E.: Anthropogenic land use estimates for the Holocene - HYDE 3.2, Earth System Science Data, 9, 927-953, 10.5194/essd-9-927-2017, 2017.

Groffman, P. M., Hardy, J. P., Driscoll, C. T., and Fahey, T. J.: Snow depth, soil freezing, and fluxes of carbon dioxide, nitrous oxide and methane in a northern hardwood forest, Global Change Biol., 12, 1748-1760, 10.1111/j.1365-2486.2006.01194.x, 2006.

Gu, J., Zheng, X., and Zhang, W.: Background nitrous oxide emissions from croplands in China in the year 2000, Plant Soil, 320, 307-320, 10.1007/s11104-009-9896-1, 2009.

Gu, J., Nicoullaud, B., Rochette, P., Grossel, A., Henault, C., Cellier, P., and Richard, G.: A regional experiment suggests that soil texture is a major control of N2O emissions from tile-drained winter wheat fields during the fertilization period, Soil Biology & Biochemistry, 60, 134-141, 10.1016/j.soilbio.2013.01.029, 2013.

Guo, J. H., Liu, X. J., Zhang, Y., Shen, J. L., Han, W. X., Zhang, W. F., Christie, P., Goulding, K. W. T., Vitousek, P. M., and Zhang, F. S.: Significant Acidification in Major Chinese Croplands, Science, 327, 1008-1010, 10.1126/science.1182570, 2010.

Guo, Y., Luo, L., Chen, G., Kou, Y., and Xu, H.: Mitigating nitrous oxide emissions from a maize-cropping black soil in northeast China by a combination of reducing chemical N fertilizer application and applying manure in autumn, Soil Science and Plant Nutrition, 59, 392-402, 10.1080/00380768.2013.775006, 2013.

Hall, S. J., McDowell, W. H., and Silver, W. L.: When Wet Gets Wetter: Decoupling of Moisture, Redox Biogeochemistry, and Greenhouse Gas Fluxes in a Humid Tropical Forest Soil, Ecosystems, 16, 576-589, 10.1007/s10021-012-9631-2, 2013.

https://doi.org/10.5194/gmd-2021-23
Preprint. Discussion started: 20 April 2021

Hayakawa, A., Akiyama, H., Sudo, S., and Yagi, K.: N2O and NO emissions from an Andisol field as influenced by pelleted poultry manure, Soil Biology & Biochemistry, 41, 521-529, 10.1016/j.soilbio.2008.12.011, 2009.

Heinen, M.: Simplified denitrification models: Overview and properties, Geoderma, 133, 444-463, 10.1016/j.geoderma.2005.06.010, 2006.

Heller, H., Bar-Tal, A., Tamir, G., Bloom, P., Venterea, R. T., Chen, D., Zhang, Y., Clapp, C. E., and Fine, P.: Effects of Manure and Cultivation on Carbon Dioxide and Nitrous Oxide Emissions from a Corn Field under Mediterranean Conditions, Journal of Environmental Quality, 39, 437-448, 10.2134/jeq2009.0027, 2010.

Hoben, J. P., Gehl, R. J., Millar, N., Grace, P. R., and Robertson, G. P.: Nonlinear nitrous oxide (N2O) response to nitrogen fertilizer in on-farm corn crops of the US Midwest, Global Change Biol., 17, 1140-1152, 10.1111/j.1365-2486.2010.02349.x, 2011.

Hunt, D. E., Bittman, S., Zhang, H., Bhandral, R., Grant, C. A., and Lemke, R.: Effect of polymer-coated urea on nitrous oxide emission in zero-till and conventionally tilled silage corn, Canadian Journal of Soil Science, 96, 12-22, 10.1139/cjss-2015-0071, 2016.

Ito, A., Nishina, K., Ishijima, K., Hashimoto, S., and Inatomi, M.: Emissions of nitrous oxide (N2O) from soil surfaces and their historical changes in East Asia: a model-based assessment, Progress in Earth and Planetary Science, 5, 10.1186/s40645-018-0215-4, 2018.

Jain, N., Arora, P., Tomer, R., Mishra, S. V., Bhatia, A., Pathak, H., Chakraborty, D., Kumar, V., Dubey, D. S., Harit, R. C., and Singha, J. P.: Greenhouse gases emission from soils under major crops in Northwest India, Science of the Total Environment, 542, 551-561, 10.1016/j.scitotenv.2015.10.073, 2016.

Jiang, G., Zhang, W., Xu, M., Kuzyakov, Y., Zhang, X., Wang, J., Di, J., and Murphy, D. V.: Manure and Mineral Fertilizer Effects on Crop Yield and Soil Carbon Sequestration: A Meta-Analysis and Modeling Across China, Global Biogeochemical Cycles, 32, 1659-1672, 10.1029/2018gb005960, 2018.

Kavdir, Y., Hellebrand, H. J., and Kern, J.: Seasonal variations of nitrous oxide emission in relation to nitrogen fertilization and energy crop types in sandy soil, Soil & Tillage Research, 98, 175-186, 10.1016/j.still.2007.11.002, 2008.

Khalil, K., Mary, B., and Renault, P.: Nitrous oxide production by nitrification and denitrification in soil aggregates as affected by O-2 concentration, Soil Biology & Biochemistry, 36, 687-699, 10.1016/j.soilbio.2004.01.004, 2004.

Kim, D. G., Vargas, R., Bond-Lamberty, B., and Turetsky, M. R.: Effects of soil rewetting and thawing on soil gas fluxes: a review of current literature and suggestions for future research, Biogeosciences, 9, 2459-2483, 10.5194/bg-9-2459-2012, 2012.

Kronzucker, H. J., Siddiqi, M. Y., and Glass, A. D. M.: Conifer root discrimination against soil nitrate and the ecology of forest succession, Nature, 385, 59-61, 10.1038/385059a0, 1997.

https://doi.org/10.5194/gmd-2021-23
Preprint. Discussion started: 20 April 2021

Kucharik, C. J., Foley, J. A., Delire, C., Fisher, V. A., Coe, M. T., Lenters, J. D., Young-Molling, C., Ramankutty, N., Norman, J. M., and Gower, S. T.: Testing the performance of a Dynamic Global Ecosystem Model: Water balance, carbon balance, and vegetation structure, Global Biogeochemical Cycles, 14, 795-825, 10.1029/1999gb001138, 2000.

Lammirato, C., Lebender, U., Tierling, J., and Lammel, J.: Analysis of uncertainty for N2O fluxes measured with the closed-chamber method under field conditions: Calculation method, detection limit, and spatial variability, J. Plant Nutr. Soil Sci., 181, 78-89, 10.1002/jpln.201600499, 2018.

Lelieveld, J., and Dentener, F. J.: What controls tropospheric ozone?, Journal of Geophysical Research-Atmospheres, 105, 3531-3551, 10.1029/1999jd901011, 2000.

Lenka, S., Lenka, N. K., Singh, A. B., Singh, B., and Raghuwanshi, J.: Global warming potential and greenhouse gas emission under different soil nutrient management practices in soybean- wheat system of central India, Environmental Science and Pollution Research, 24, 4603-4612, 10.1007/s11356-016-8189-5, 2017.

Li, C. S., Aber, J., Stange, F., Butterbach-Bahl, K., and Papen, H.: A process-oriented model of N2O and NO emissions from forest soils: 1. Model development, Journal of Geophysical Research-Atmospheres, 105, 4369-4384, 10.1029/1999jd900949, 2000.

Li, H., Qiu, J., Wang, L., Tang, H., Li, C., and Van Ranst, E.: Modelling impacts of alternative farming management practices on greenhouse gas emissions from a winter wheat-maize rotation system in China, Agriculture Ecosystems & Environment, 135, 24-33, 10.1016/j.agee.2009.08.003, 2010.

Li, Y., Barton, L., and Chen, D.: Simulating response of N2O emissions to fertiliser N application and climatic variability from a rain-fed and wheat-cropped soil in Western Australia, Journal of the Science of Food and Agriculture, 92, 1130-1143, 10.1002/jsfa.4643, 2012.

Li, Z., Zeng, Z., Tian, D., Wang, J., Fu, Z., Zhang, F., Zhang, R., Chen, W., Luo, Y., and Niu, S.: Global patterns and controlling factors of soil nitrification rate, Global Change Biol., 10.1111/gcb.15119, 2020.

Lin, S., Iqbal, J., Hu, R., Ruan, L., Wu, J., Zhao, J., and Wang, P.: Differences in nitrous oxide fluxes from red soil under different land uses in mid-subtropical China, Agriculture Ecosystems & Environment, 146, 168-178, 10.1016/j.agee.2011.10.024, 2012.

Liu, C., Lu, M., Cui, J., Li, B., and Fang, C.: Effects of straw carbon input on carbon dynamics in agricultural soils: a meta-analysis, Global Change Biol., 20, 1366-1381, 10.1111/gcb.12517, 2014.

Liu, J., You, L., Amini, M., Obersteiner, M., Herrero, M., Zehnder, A. J. B., and Yang, H.: A high-resolution assessment on global nitrogen flows in cropland, Proceedings of the National Academy of Sciences, 107, 8035-8040, 10.1073/pnas.0913658107, 2010.

https://doi.org/10.5194/gmd-2021-23
Preprint. Discussion started: 20 April 2021

Lognoul, M., Debacq, A., De Ligne, A., Dumont, B., Manise, T., Bodson, B., Heinesch, B., and Aubinet, M.: N2O flux short-term response to temperature and topsoil disturbance in a fertilized crop: An eddy covariance campaign, Agricultural and Forest Meteorology, 271, 193-206, 10.1016/j.agrformet.2019.02.033, 2019.

Lugato, E., Zuliani, M., Alberti, G., Delle Vedove, G., Gioli, B., Miglietta, F., and Peressotti, A.: Application of DNDC biogeochemistry model to estimate greenhouse gas emissions from Italian agricultural areas at high spatial resolution, Agriculture Ecosystems & Environment, 139, 546-556, 10.1016/j.agee.2010.09.015, 2010.

Malhi, S. S., Nyborg, M., Jahn, H. G., and Penney, D. C.: Yield and nitrogen uptake of rapessed (Brassica campestris L.) with ammonium and nitrate, Plant Soil, 105, 231-239, 10.1007/BF02376787, 1988.

Maris, S. C., Teira-Esmatges, M. R., Arbones, A., and Rufat, J.: Effect of irrigation, nitrogen application, and a nitrification inhibitor on nitrous oxide, carbon dioxide and methane emissions from an olive (Olea europaea L.) orchard, Sci. Total Environ., 538, 966-978, 10.1016/j.scitotenv.2015.08.040, 2015.

Mei, K., Wang, Z., Huang, H., Zhang, C., Shang, X., Dahlgren, R. A., Zhang, M., and Xia, F.: Stimulation of N2O emission by conservation tillage management in agricultural lands: A meta-analysis, Soil & Tillage Research, 182, 86-93, 10.1016/j.still.2018.05.006, 2018.

Meijide, A., Díez, J. A., Sánchez-Martín, L., López-Fernández, S., and Vallejo, A.: Nitrogen oxide emissions from an irrigated maize crop amended with treated pig slurries and composts in a Mediterranean climate, Agriculture Ecosystems & Environment, 121, 383-394, 2007.

Meng, L., Ding, W. X., and Cai, Z. C.: Long-term application of organic manure and nitrogen fertilizer on N2O emissions, soil quality and crop production in a sandy loam soil, Soil Biology & Biochemistry, 37, 2037-2045, 10.1016/j.soilbio.2005.03.007, 2005.

Monfreda, C., Ramankutty, N., and Foley, J. A.: Farming the planet: 2. Geographic distribution of crop areas, yields, physiological types, and net primary production in the year 2000, Global Biogeochemical Cycles, 22, 10.1029/2007gb002947, 2008.

Morkved, P. T., Dorsch, P., and Bakken, L. R.: The N2O product ratio of nitrification and its dependence on long-term changes in soil pH, Soil Biology & Biochemistry, 39, 2048-2057, 10.1016/j.soilbio.2007.03.006, 2007.

Mosier, A. R., Halvorson, A. D., Reule, C. A., and Liu, X. J.: Net global warming potential and greenhouse gas intensity in irrigated cropping systems in northeastern Colorado, Journal of Environmental Quality, 35, 1584-1598, 10.2134/jeq2005.0232, 2006.

Nishina, K., Ito, A., Hanasaki, N., and Hayashi, S.: Reconstruction of spatially detailed global map of NH4+ and NO3- application in synthetic nitrogen fertilizer, Earth System Science Data, 9, 149-162, 10.1594/pangaea.861203, 2017.

https://doi.org/10.5194/gmd-2021-23
Preprint. Discussion started: 20 April 2021

Norman, J., Jansson, P.-E., Farahbakhshazad, N., Butterbach-Bahl, K., Li, C., and Klemedtsson, L.: Simulation of NO and N2O emissions from a spruce forest during a freeze/thaw event using an N-flux submodel from the PnET-N-DNDC model integrated to CoupModel, Ecol. Model., 216, 18-30, 10.1016/j.ecolmodel.2008.04.012, 2008.

Oehler, F., Rutherford, J. C., and Coco, G.: The use of machine learning algorithms to design a generalized simplified denitrification model, Biogeosciences, 7, 3311-3332, 10.5194/bg-7-3311-2010, 2010.

Ogle, S. M., Alsaker, C., Baldock, J., Bernoux, M., Breidt, F. J., McConkey, B., Regina, K., and Vazquez-Amabile, G. G.: Climate and Soil Characteristics Determine Where No-Till Management Can Store Carbon in Soils and Mitigate Greenhouse Gas Emissions, Scientific Reports, 9, 10.1038/s41598-019-47861-7, 2019.

Parton, W. J., Mosier, A. R., Ojima, D. S., Valentine, D. W., and Kulmala, A. E.: Generalized model for N2 and N2O production from nitrification and denitrification, Global Biogeochemical Cycles, 10, 401-412, 1996.

Passianoto, C. C., Ahrens, T., Feigl, B. J., Steudler, P. A., do Carmo, J. B., and Melillo, J. M.: Emissions of CO(2), N(2)O, and NO in conventional and no-till management practices in Rondonia, Brazil, Biology and Fertility of Soils, 38, 200-208, 10.1007/s00374-003-0653-y, 2003.

Peng, C., Zhu, Q., and Chen, H.: Integrating greenhouse gas emission processes into a dynamic global vegetation model of TRIPLEX-GHG, Egu General Assembly Conference, 2013,

Peng, C. H., Liu, J. X., Dang, Q. L., Apps, M. J., and Jiang, H.: TRIPLEX: a generic hybrid model for predicting forest growth and carbon and nitrogen dynamics, Ecol. Model., 153, 109-130, 10.1016/s0304-3800(01)00505-1, 2002.

Perlman, J., Hijmans, R. J., and Horwath, W. R.: A metamodelling approach to estimate global N2O emissions from agricultural soils, Global Ecol. Biogeogr., 23, 912-924, 10.1111/geb.12166, 2014.

Petersen, S. O., Regina, K., Pollinger, A., Rigler, E., Valli, L., Yamulki, S., Esala, M., Fabbri, C., Syvasalo, E., and Vinther, F. P.: Nitrous oxide emissions from organic and conventional crop rotations in five European countries, Agriculture Ecosystems & Environment, 112, 200-206, 10.1016/j.agee.2005.08.021, 2006.

Pfab, H., Palmer, I., Buegger, F., Fiedler, S., Mueller, T., and Ruser, R.: Influence of a nitrification inhibitor and of placed N-fertilization on N2O fluxes from a vegetable cropped loamy soil, Agriculture Ecosystems & Environment, 150, 91-101, 10.1016/j.agee.2012.01.001, 2012.

Philibert, A., Loyce, C., and Makowski, D.: Prediction of N2O emission from local information with Random Forest, Environ. Pollut., 177, 156-163, 10.1016/j.envpol.2013.02.019, 2013.

Potter, C. S., Matson, P. A., Vitousek, P. M., and Davidson, E. A.: Process modeling of controls on nitrogen trace gas emissions from soils worldwide, Journal of Geophysical Research-Atmospheres, 101, 1361-1377, 10.1029/95jd02028, 1996.

Powlson, D. S., Stirling, C. M., Jat, M. L., Gerard, B. G., Palm, C. A., Sanchez, P. A., and Cassman, K. G.: Limited potential of no-till agriculture for climate change mitigation, Nature Climate Change, 4, 678-683, 10.1038/nclimate2292, 2014.

https://doi.org/10.5194/gmd-2021-23
Preprint. Discussion started: 20 April 2021

Rabot, E., Cousin, I., and Henault, C.: A modeling approach of the relationship between nitrous oxide fluxes from soils and the water-filled pore space, Biogeochemistry, 122, 395-408, 10.1007/s10533-014-0048-1, 2015.

Rochette, P.: No-till only increases N2O emissions in poorly-aerated soils, Soil & Tillage Research, 101, 97-100, 10.1016/j.still.2008.07.011, 2008.

Rochette, P., Angers, D. A., Chantigny, M. H., Gagnon, B., and Bertrand, N.: N2O fluxes in soils of contrasting textures fertilized with liquid and solid dairy cattle manures, Canadian Journal of Soil Science, 88, 175-187, 10.4141/cjss06016, 2008.

Rochette, P., Liang, C., Pelster, D., Bergeron, O., Lemke, R., Kroebel, R., MacDonald, D., Yan, W., and Flemming, C.: Soil nitrous oxide emissions from agricultural soils in Canada: Exploring relationships with soil, crop and climatic variables, Agriculture Ecosystems & Environment, 254, 69-81, 10.1016/j.agee.2017.10.021, 2018.

Rosenstock, T. S., Mpanda, M., Pelster, D. E., Butterbach-Bahl, K., Rufino, M. C., Thiong'o, M., Mutuo, P., Abwanda, S., Rioux, J., Kimaro, A. A., and Neufeldt, H.: Greenhouse gas fluxes from agricultural soils of Kenya and Tanzania, Journal of Geophysical Research-Biogeosciences, 121, 1568-1580, 10.1002/2016jg003341, 2016.

Rowlings, D. W., Grace, P. R., Scheer, C., and Kiese, R.: Influence of nitrogen fertiliser application and timing on greenhouse gas emissions from a lychee (Litchi chinensis) orchard in humid subtropical Australia, Agriculture Ecosystems & Environment, 179, 168-178, 10.1016/j.agee.2013.08.013, 2013.

Sacks, W. J., Deryng, D., Foley, J. A., and Ramankutty, N.: Crop planting dates: an analysis of global patterns, Global Ecol. Biogeogr., 19, 607-620, 10.1111/j.1466-8238.2010.00551.x, 2010.

Saikawa, E., Schlosser, C. A., and Prinn, R. G.: Global modeling of soil nitrous oxide emissions from natural processes, Global Biogeochemical Cycles, 27, 972-989, 10.1002/gbc.20087, 2013.

Sanchez-Martin, L., Arce, A., Benito, A., Garcia-Torres, L., and Vallejo, A.: Influence of drip and furrow irrigation systems on nitrogen oxide emissions from a horticultural crop, Soil Biology & Biochemistry, 40, 1698-1706, 10.1016/j.soilbio.2008.02.005, 2008.

Sanchez, C., and Minamisawa, K.: Nitrogen Cycling in Soybean Rhizosphere: Sources and Sinks of Nitrous Oxide (N2O), Frontiers in Microbiology, 10, 10.3389/fmicb.2019.01943, 2019.

Sanz-Cobena, A., Sanchez-Martin, L., Garcia-Torres, L., and Vallejo, A.: Gaseous emissions of N2O and NO and NO3- leaching from urea applied with urease and nitrification inhibitors to a maize (Zea mays) crop, Agriculture Ecosystems & Environment, 149, 64-73, 10.1016/j.agee.2011.12.016, 2012.

Scheer, C., Wassmann, R., Kienzler, K., Ibragimov, N., Lamers, J. P. A., and Martius, C.: Methane and nitrous oxide fluxes in annual and perennial land-use systems of the irrigated areas in the Aral Sea Basin, Global Change Biology, 14, 2454-2468, 10.1111/j.1365-2486.2008.01631.x, 2008.

https://doi.org/10.5194/gmd-2021-23
Preprint. Discussion started: 20 April 2021

Scheer, C., Grace, P. R., Rowlings, D. W., and Payero, J.: Nitrous oxide emissions from irrigated wheat in Australia: impact of irrigation management, Plant and Soil, 359, 351-362, 10.1007/s11104-012-1197-4, 2012.

Scheer, C., Grace, P. R., Rowlings, D. W., and Payero, J.: Soil N2O and CO2 emissions from cotton in Australia under varying irrigation management, Nutrient Cycling in Agroecosystems, 95, 43-56, 10.1007/s10705-012-9547-4, 2013.

Scheer, C., Rowlings, D. W., and Grace, P. R.: Non-linear response of soil N2O emissions to nitrogen fertiliser in a cotton-fallow rotation in sub-tropical Australia, Soil Research, 54, 494-499, 10.1071/sr14328, 2016.

Sebilo, M., Mayer, B., Nicolardot, B., Pinay, G., and Mariotti, A.: Long-term fate of nitrate fertilizer in agricultural soils, Proceedings of the National Academy of Sciences of the United States of America, 110, 18185-18189, 10.1073/pnas.1305372110, 2013.

Senapati, N., Chabbi, A., Giostri, A. F., Yeluripati, J. B., and Smith, P.: Modelling nitrous oxide emissions from mown-grass and grain-cropping systems: Testing and sensitivity analysis of DailyDayCent using high frequency measurements, Science of the Total Environment, 572, 955-977, 10.1016/j.scitotenv.2016.07.226, 2016.

Shan, J., and Yan, X.: Effects of crop residue returning on nitrous oxide emissions in agricultural soils, Atmos. Environ., 71, 170-175, 10.1016/j.atmosenv.2013.02.009, 2013.

Sharma, S., Szele, Z., Schilling, R., Munch, J. C., and Schloter, M.: Influence of freeze-thaw stress on the structure and function of microbial communities and denitrifying populations in soil, Appl. Environ. Microbiol., 72, 2148-2154, 10.1128/aem.72.3.2148-2154.2006, 2006.

Shcherbak, I., Millar, N., and Robertson, G. P.: Global metaanalysis of the nonlinear response of soil nitrous oxide (N2O) emissions to fertilizer nitrogen, Proceedings of the National Academy of Sciences of the United States of America, 111, 9199-9204, 10.1073/pnas.1322434111, 2014.

Snyder, C. S., Bruulsema, T. W., Jensen, T. L., and Fixen, P. E.: Review of greenhouse gas emissions from crop production systems and fertilizer management effects, Agriculture Ecosystems & Environment, 133, 247-266, 10.1016/j.agee.2009.04.021, 2009.

Soares, J. R., Cantarella, H., Vargas, V. P., Carmo, J. B., Martins, A. A., Sousa, R. M., and Andrade, C. A.: Enhanced-Efficiency Fertilizers in Nitrous Oxide Emissions from Urea Applied to Sugarcane, Journal of Environmental Quality, 44, 423-430, 10.2134/jeq2014.02.0096, 2015.

Song, X., Ju, X., Topp, C. F. E., and Rees, R. M.: Oxygen Regulates Nitrous Oxide Production Directly in Agricultural Soils, Environ. Sci. Technol., 53, 12539-12547, 10.1021/acs.est.9b03089, 2019.

Sosulski, T., Szara, E., Stepien, W., and Rutkowska, B.: The influence of mineral fertilization and legumes cultivation on the N2O soil emissions, Plant Soil and Environment, 61, 529-536, 10.17221/229/2015-pse, 2015.

https://doi.org/10.5194/gmd-2021-23
Preprint. Discussion started: 20 April 2021

Stehfest, E., and Bouwman, L.: N2O and NO emission from agricultural fields and soils under natural vegetation: summarizing available measurement data and modeling of global annual emissions, Nutrient Cycling in Agroecosystems, 74, 207-228, 10.1007/s10705-006-9000-7, 2006.

Teepe, R., Vor, A., Beese, F., and Ludwig, B.: Emissions of N2O from soils during cycles of freezing and thawing and the effects of soil water, texture and duration of freezing, Eur. J. Soil Sci., 55, 357-365, 10.1111/j.1365-2389.2004.00602.x, 2004.

Thorburn, P. J., Biggs, J. S., Collins, K., and Probert, M. E.: Using the APSIM model to estimate nitrous oxide emissions from diverse Australian sugarcane production systems, Agriculture Ecosystems & Environment, 136, 343-350, 10.1016/j.agee.2009.12.014, 2010.

Tian, D., and Niu, S.: A global analysis of soil acidification caused by nitrogen addition, Environmental Research Letters, 10, 10.1088/1748-9326/10/2/024019, 2015.

Tian, H., Xu, X., Liu, M., Ren, W., Zhang, C., Chen, G., and Lu, C.: Spatial and temporal patterns of CH4 and N2O fluxes in terrestrial ecosystems of North America during 1979-2008: application of a global biogeochemistry model, Biogeosciences, 7, 2673-2694, 10.5194/bg-7-2673-2010, 2010.

Tian, H., Chen, G., Lu, C., Xu, X., Hayes, D. J., Ren, W., Pan, S., Huntzinger, D. N., and Wofsy, S. C.: North American terrestrial CO2 uptake largely offset by CH4 and N2O emissions: toward a full accounting of the greenhouse gas budget, Clim. Change, 129, 413-426, 10.1007/s10584-014-1072-9, 2015.

Tian, H., Lu, C., Ciais, P., Michalak, A. M., Canadell, J. G., Saikawa, E., Huntzinger, D. N., Gurney, K. R., Sitch, S., Zhang, B., Yang, J., Bousquet, P., Bruhwiler, L., Chen, G., Dlugokencky, E., Friedlingstein, P., Melillo, J., Pan, S., Poulter, B., Prinn, R., Saunois, M., Schwalm, C. R., and Wofsy, S. C.: The terrestrial biosphere as a net source of greenhouse gases to the atmosphere, Nature, 531, 225-+, 10.1038/nature16946, 2016.

Tian, H., Yang, J., Lu, C., Xu, R., Canadell, J. G., Jackson, R. B., Arneth, A., Chang, J., Chen, G., Ciais, P., Gerber, S., Ito, A., Huang, Y., Joos, F., Lienert, S., Messina, P., Olin, S., Pan, S., Peng, C., Saikawa, E., Thompson, R. L., Vuichard, N., Winiwarter, W., Zaehle, S., Zhang, B., Zhang, K., and Zhu, Q.: The Global N2O Model Intercomparison Project, Bulletin of the American Meteorological Society, 99, 1231-1251, 10.1175/bams-d-17-0212.1, 2018.

Tian, H., Yang, J., Xu, R., Lu, C., Canadell, J. G., Davidson, E. A., Jackson, R. B., Arneth, A., Chang, J., Ciais, P., Gerber, S., Ito, A., Joos, F., Lienert, S., Messina, P., Olin, S., Pan, S., Peng, C., Saikawa, E., Thompson, R. L., Vuichard, N., Winiwarter, W., Zaehle, S., and Zhang, B.: Global soil nitrous oxide emissions since the preindustrial era estimated by an ensemble of terrestrial biosphere models: Magnitude, attribution, and uncertainty, Global Change Biol., 25, 640-659, 10.1111/gcb.14514, 2019.

Tian, H., Xu, R., Canadell, J. G., Thompson, R. L., Winiwarter, W., Suntharalingam, P., Davidson, E. A., Ciais, P., Jackson, R. B., Janssens-Maenhout, G., Prather, M. J., Regnier, P., Pan, N., Pan, S., Peters, G. P., Shi, H., Tubiello, F. N., Zaehle, S., Zhou,

https://doi.org/10.5194/gmd-2021-23
Preprint. Discussion started: 20 April 2021

F., Arneth, A., Battaglia, G., Berthet, S., Bopp, L., Bouwman, A. F., Buitenhuis, E. T., Chang, J., Chipperfield, M. P., Dangal, S. R. S., Dlugokencky, E., Elkins, J. W., Eyre, B. D., Fu, B., Hall, B., Ito, A., Joos, F., Krummel, P. B., Landolfi, A., Laruelle, G. G., Lauerwald, R., Li, W., Lienert, S., Maavara, T., MacLeod, M., Millet, D. B., Olin, S., Patra, P. K., Prinn, R. G., Raymond, P. A., Ruiz, D. J., van der Werf, G. R., Vuichard, N., Wang, J., Weiss, R. F., Wells, K. C., Wilson, C., Yang, J., and Yao, Y.: A comprehensive quantification of global nitrous oxide sources and sinks, Nature, 586, 248-256, 10.1038/s41586-020-2780-0, 2020.

van Aardenne, J. A., Dentener, F. J., Olivier, J. G. J., Goldewijk, C., and Lelieveld, J.: A 1 degrees x 1 degrees resolution data set of historical anthropogenic trace gas emissions for the period 1890-1990, Global Biogeochemical Cycles, 15, 909-928, 10.1029/2000gb001265, 2001.

van Kessel, C., Venterea, R., Six, J., Adviento-Borbe, M. A., Linquist, B., and van Groenigen, K. J.: Climate, duration, and N placement determine N2O emissions in reduced tillage systems: a meta-analysis, Global Change Biol., 19, 33-44, 10.1111/j.1365-2486.2012.02779.x, 2013.

Venterea, R. T., Maharjan, B., and Dolan, M. S.: Fertilizer Source and Tillage Effects on Yield-Scaled Nitrous Oxide Emissions in a Corn Cropping System, Journal of Environmental Quality, 40, 1521-1531, 10.2134/jeq2011.0039, 2011.

VERHOEVEN, Elizabeth, and Johan: Biochar does not mitigate field-scale N2O emissions in a Northern California vineyard: An assessment across two years, Agriculture Ecosystems & Environment, 191, 27-38, 2014.

Wagner-Riddle, C., Congreves, K. A., Abalos, D., Berg, A. A., Brown, S. E., Ambadan, J. T., Gao, X., and Tenuta, M.: Globally important nitrous oxide emissions from croplands induced by freeze-thaw cycles, Nature Geoscience, 10, 279-+, 10.1038/ngeo2907, 2017.

Wang, J., Chadwick, D. R., Cheng, Y., and Yan, X.: Global analysis of agricultural soil denitrification in response to fertilizer nitrogen, Sci. Total Environ., 616, 908-917, 10.1016/j.scitotenv.2017.10.229, 2018a.

Wang, K., Zheng, X., Pihlatie, M., Vesala, T., Liu, C., Haapanala, S., Mammarella, I., Rannik, U., and Liu, H.: Comparison between static chamber and tunable diode laser-based eddy covariance techniques for measuring nitrous oxide fluxes from a cotton field, Agricultural and Forest Meteorology, 171, 9-19, 10.1016/j.agrformet.2012.11.009, 2013.

Wang, W., Dalal, R. C., Reeves, S. H., Butterbach-Bahl, K., and Kiese, R.: Greenhouse gas fluxes from an Australian subtropical cropland under long-term contrasting management regimes, Global Change Biology, 17, 3089-3101, 10.1111/j.1365-2486.2011.02458.x, 2011.

Wang, Y., Guo, J., Vogt, R. D., Mulder, J., Wang, J., and Zhang, X.: Soil pH as the chief modifier for regional nitrous oxide emissions: New evidence and implications for global estimates and mitigation, Global Change Biol., 24, E617-E626, 10.1111/gcb.13966, 2018b.

https://doi.org/10.5194/gmd-2021-23
Preprint. Discussion started: 20 April 2021

Wania, R., Ross, I., and Prentice, I. C.: Implementation and evaluation of a new methane model within a dynamic global vegetation model: LPJ-WHyMe v1.3.1, Geoscientific Model Development, 3, 565-584, 10.5194/gmd-3-565-2010, 2010.

Wanyama, I., Pelster, D. E., Arias-Navarro, C., Butterbach-Bahl, K., Verchot, L. V., and Rufino, M. C.: Management intensity controls soil N2O fluxes in an Afromontane ecosystem, Sci. Total Environ., 624, 769-780, 10.1016/j.scitotenv.2017.12.081, 2018.

Willmott, C. J.: On the Validation of Model, Physical Geography, 2, 219-232, 1981.

Wolf, B., Zheng, X., Brüggemann, N., Chen, W., Dannenmann, M., Han, X., Sutton, M. A., Wu, H., Yao, Z., and Butterbach-Bahl, K.: Grazing-induced reduction of natural nitrous oxide release from continental steppe, Nature, 464, 881-884, 10.1038/nature08931, 2010.

Wrage-Moennig, N., Horn, M. A., Well, R., Mueller, C., Velthof, G., and Oenema, O.: The role of nitrifier denitrification in the production of nitrous oxide revisited, Soil Biology & Biochemistry, 123, A3-A16, 10.1016/j.soilbio.2018.03.020, 2018.

Wrage, N., Velthof, G. L., van Beusichem, M. L., and Oenema, O.: Role of nitrifier denitrification in the production of nitrous oxide, Soil Biology & Biochemistry, 33, 1723-1732, 10.1016/s0038-0717(01)00096-7, 2001.

Xu, R., and Prentice, I. C.: Terrestrial nitrogen cycle simulation with a dynamic global vegetation model, Global Change Biol., 14, 1745-1764, 10.1111/j.1365-2486.2008.01625.x, 2008.

Xu, R., Prentice, I. C., Spahni, R., and Niu, H. S.: Modelling terrestrial nitrous oxide emissions and implications for climate feedback, New Phytol., 196, 472-488, 10.1111/j.1469-8137.2012.04269.x, 2012.

Xu, R., Tian, H., Lu, C., Pan, S., Chen, J., Yang, J., and Zhang, B.: Preindustrial nitrous oxide emissions from the land biosphere estimated by using a global biogeochemistry model, Climate of the Past, 13, 977-990, 10.5194/cp-13-977-2017, 2017.

Yang, L. F., and Cai, Z. C.: The effect of growing soybean (Glycine max. L.) on N2O emission from soil, Soil Biology & Biochemistry, 37, 1205-1209, 10.1016/j.soilbio.2004.08.027, 2005.

Zebarth, B. J., Snowdon, E., Burton, D. L., Goyer, C., and Dowbenko, R.: Controlled release fertilizer product effects on potato crop response and nitrous oxide emissions under rain-fed production on a medium-textured soil, Canadian Journal of Soil Science, 92, 759-769, 10.4141/cjss2012-008, 2012.

Zhang, B., Tian, H., Lu, C., Dangal, S. R. S., Yang, J., and Pan, S.: Global manure nitrogen production and application in cropland during 1860-2014: a 5 arcmin gridded global dataset for Earth system modeling, Earth System Science Data, 9, 667-678, 10.5194/essd-9-667-2017, 2017a.

Zhang, K., Peng, C., Wang, M., Zhou, X., Li, M., Wang, K., Ding, J., and Zhu, Q.: Process-based TRIPLEX-GHG model for simulating N2O emissions from global forests and grasslands: Model development and evaluation, Journal of Advances in Modeling Earth Systems, 9, 2079-2102, 10.1002/2017ms000934, 2017b.

https://doi.org/10.5194/gmd-2021-23
Preprint. Discussion started: 20 April 2021

Zhang, K., Zhu, Q., Liu, J., Wang, M., Zhou, X., Li, M., Wang, K., Ding, J., and Peng, C.: Spatial and temporal variations of N2O emissions from global forest and grassland ecosystems, Agricultural and Forest Meteorology, 266, 129-139, 10.1016/j.agrformet.2018.12.011, 2019.

Zhang, Y., Lin, F., Jin, Y., Wang, X., Liu, S., and Zou, J.: Response of nitric and nitrous oxide fluxes to N fertilizer application in greenhouse vegetable cropping systems in southeast China, Scientific Reports, 6, 10.1038/srep20700, 2016.

Zhou, M., Zhu, B., Wang, S., Zhu, X., Vereecken, H., and Brueggemann, N.: Stimulation of N2O emission by manure application to agricultural soils may largely offset carbon benefits: a global meta-analysis, Global Change Biol., 23, 4068-4083, 10.1111/gcb.13648, 2017.

Zhou, M., Wang, X., Ke, Y., and Zhu, B.: Effects of afforestation on soil nitrous oxide emissions in a subtropical montane agricultural landscape: A 3-year field experiment, Agricultural and Forest Meteorology, 266, 221-230, 10.1016/j.agrformet.2019.01.003, 2019.

Zhu, Q., Liu, J., Peng, C., Chen, H., Fang, X., Jiang, H., Yang, G., Zhu, D., Wang, W., and Zhou, X.: Modelling methane emissions from natural wetlands by development and application of the TRIPLEX-GHG model, Geoscientific Model Development, 7, 981-999, 10.5194/gmd-7-981-2014, 2014.

Zhu, Q., Peng, C., Chen, H., Fang, X., Liu, J., Jiang, H., Yang, Y., and Yang, G.: Estimating global natural wetland methane emissions using process modelling: spatio-temporal patterns and contributions to atmospheric methane fluctuations, Global Ecol. Biogeogr., 24, 959-972, 10.1111/geb.12307, 2015.

Zhu, X., Burger, M., Doane, T. A., and Horwath, W. R.: Ammonia oxidation pathways and nitrifier denitrification are significant sources of N₂O and NO under low oxygen availability, Proceedings of the National Academy of Sciences, 110, 6328-6333, 10.1073/pnas.1219993110, 2013.

https://doi.org/10.5194/gmd-2021-23
Preprint. Discussion started: 20 April 2021

Geoscientific Model Development Discussions

Table.1 List of the major parameters for processes associated with N_2O production.

Parameters	Explanation	Values	Unit	References
COE_{dNO3}	Coefficient for consumption rate of NO_3^-	0.05		(Li et al., 2000; Zhang et al., 2017a)
COE_{NR}	Nitrification rate coefficient	0.044		(Cai et al., 2014; Zhang et al., 2017a)
NMUEMAX	Growth coefficient for nitrifiers	0.102	d^{-1}	(Li et al., 2000)
AMAX	Mortality coefficient for nitrifiers	0.06	d^{-1}	(Li et al., 2000)
MUE_{NO3}	Maximum growth rate of NO_3^- denitrifiers	0.67	h^{-1}	(Li et al., 2000)
MUE_{NO2}	Maximum growth rate of NO_2^- denitrifiers	0.67	h^{-1}	(Li et al., 2000)
MUE_{N2O}	Maximum growth rate of N_2O denitrifiers	0.47	h^{-1}	(Li et al., 2000)
EFF_{NO3}	Efficiency parameter for NO_3^- denitrifiers	0.501	h^{-1}	(Li et al., 2000)
EFF_{NO2}	Efficiency parameter for NO_2^- Denitrifiers	0.428	h^{-1}	(Li et al., 2000)
EFF_{N2O}	Efficiency parameter for N_2O denitrifiers	0.075	h^{-1}	(Li et al., 2000)
M_{NO3}	Maintenance coefficient on NO_3^-	0.09	h^{-1}	(Li et al., 2000) Leffelaar, and Wessel 1988,
COE_{dNO2}	Coefficient for consumption rate of NO_2^-	1.0		(Norman et al., 2008; Zhang et al., 2017a)
COE_{dNO}	Coefficient for consumption rate of NO	1.0		(Norman et al., 2008; Zhang et al., 2017a)

Geoscientific Model Development Discussions
Open Access

Table 2. Information on the selected sites used for the model calibration.

ID	Sites	Lat.	Lon.	Experiment period	Crop type	Fertilization (kgN $ha^{-1}yr^{-1}$)	return straw	irrigate	clay	sand	pH	SOC (%)	Soil C:N ratio	Mean N_2O flux (mgN m^{-2} day^{-1})	Method	Reference
NA-1	Woodslee, Ontario, CA	42.1	-82.6	2003-2005	corn	150	yes	no	52.5	20	6.4	12.5	4.7	0.47	closed chamber	(Drury et al., 2008)
NA-2	Rosemount, MN, USA	44.8	-93.1	2008-2009	corn	146	no	no	23.0	22	6.2	2.8	9.4	0.25	stainless steel chamber	(Venterea et al., 2011)
NA-3	Marlboro, MD, USA	39.4	-77.3	2012-2014	Tobacco; corn	134	yes	no	9.3	79.6	6.2	0.8	9.1	1.04	static flux chamber	(Chen et al., 2018)
NA-4	Fredericton, NB, CA	45.9	-66.6	2008-2011	potato	193	no	no	11	49	6.2	1.9	14.8	0.18	non-steady-state chamber	(Zebarth et al., 2012)
NA-5	Que´bec City, CA	46.8	-71.4	2002-2003	corn	150	no	no	48.2	11.2	6.9	3.4	14.6	1.68	non-steady-state chambers	(Rochette et al., 2008b)
NA-6	Fort Collins, Colorado, USA	40.7	-105.0	2002-2005	corn	134	yes	no	33.4	40.2	7.7	1.3	8.4	0.30	automatedgas chromatograph	(Mosier et al., 2006)
NA-7	Baton Rouge, LA, USA	30.4	-91.2	2013-2014	cotton	112	no	no	20.5	34.7	6.2	6.6	9.9	4.40	closed chamber	(Tian et al., 2015)
NA-8	Sacramento County, CA	38.3	-121.5	2010-2012	grape	38	yes	yes	23	50	6.4	11.2	10.7	1.15	closed chamber	(VERHOEVEN et al., 2014)
NA-9	British	49.2	-	2005-2007	corn	150	yes	no	14	27	6.1		13.6	1.04	static flux	(Hunt et al., 2016)

https://doi.org/10.5194/gmd-2021-23
Preprint. Discussion started: 20 April 2021

Geoscientific Model Development Discussions
Open Access

AS-1	New Delhi, Inida	28.2	77.2	2008-2010	wheat	120	no	no	22	52	8.1	0.6	8.6	0.27	closed-chamber	(Jain et al., 2016)
AS-2	Gongzhuling, Jilin,China	43.5	124.8	2010-2012	maize	230	yes	no	23	39	6.2	2.6	9.0	0.72	static closed-chamber	(Guo et al., 2013)
AS-3	Yanting, Sichuan, China	31.3	105.5	2012-2015	wheat; maize	300	yes	no	19.6	30.1	8.1	1.2	8.3	0.80	static chamber	(Zhou et al., 2019)
AS-4	Nanjing, Jiangsu, China	32.1	119.0	2013-2014	vegetable	420	no	yes	54.5	15.2	5.5	1.5	8.8	3.52	static chamber	(Zhang et al., 2016)
AS-5	Yuncheng, Shanxi, China	34.9	110.7	2008-2010	Cotton	70	no	yes	37.6	16.6	8.7	1.0	7.1	0.79	Automatic chamber	(Wang et al., 2013)
AS-6	Fengqiu, Henan, China	35.0	114.3	2002-2003	maize; wheat	150	yes	no	6	79	8.7	8.9	7.9	0.23	close-chamber	(Meng et al., 2005)
AS-7	Japan	36.0	140.1	2006-2007	Komatsuna	120	no	no	21	32	5.9	10.7	8.4	0.10	automated chamber	(Hayakawa et al., 2009)
AS-8	Shandong, China	36.9	117.9	2008-2009	Maize; wheat	600	yes	yes	17.1	16.8	8.3	1.8	7.9	1.10	static chamber	(Cui et al., 2012)
AS-9	Xianning, China	29.9	114.3	2005-2007	peanut	120	yes	no	2.4	49.0	5.2	0.9	4.9	0.34	static closed chamber	(Lin et al., 2012)
AS-10	Khorezm Uzbekistan	41.6	60.5	2005-2006	Cotton; wheat	250	yes	yes	14.6	42.6	6.9	0.6	3.1	2.14	closed chamber	(Scheer et al., 2008)
EU-1	Potsdam Bornim, Germany	52.4	13.0	2003-2005	rape	150	no	no	4	87.5	6.0	0.9	14.0	1.08	static chamber	(Kavdir et al., 2008)
EU-2	Lusignan, France	46.4	0.1	2011-2014	corn; wheat	125	no	yes	17.6	13.2	6.4	13.5	10.6	0.34	Automatic chamber	(Senapati et al., 2016)

https://doi.org/10.5194/gmd-2021-23
Preprint. Discussion started: 20 April 2021

Geoscientific Model Development Discussions
Open Access

EU-3	St. Petersburg, Russia	59.6	30.1	2003-2005	potato	120	yes	no	25.5	18	5.8	1.5	8.8	1.22	closed chamber	(Buchkina et al., 2010)
EU-4	BetDagan, Israel	32.0	34.8	2006-2007	cotton	240	yes	yes	17.5	80	7.3		10.3	9.42	PVC sample chamber	(Heller et al., 2010)
EU-5	Skierniewice, Poland	52.6	20.3	2012-2013	barley	45	yes	no	7	87	6.6	11.0	11.1	0.44	closed chamber	(Sosulski et al., 2015)
EU-6	Wye Estate, UK	51.9	1.0	1999-2001	Wheat; rye	200	yes	no	15	17	5.8	1.9	8.6	6.20	closed chamber	(Baggs et al., 2003)
EU-7	Stuttgart, Germany	48.7	9.2	2008-2010	vegetable	401	no	no	30	2	5.5	1.8	8.0	1.85	PVC-chamber	(Pfab et al., 2012)
EU-8	Naples, Italy	40.6	15.0	2007-2008	maize	130	no	no	32.9	47	7.5	0.8	8.4	0.10	automated closed static chambers	(Forte et al., 2017)
EU-9	Madrid, Spain	40.5	-3.3	2009-2012	Maize; barley	250	yes	yes	28	55	7.9	0.8	8.1	0.77	closed chamber	(Abalos et al., 2013; Sanz-Cobena et al., 2012)
AU-1	Cunderdin, Australia	-31.6	117.2	2005-2007	wheat	100;75	yes	no	18.6	77.0	6.0	0.4	10.0	0.032	automated gas chambers	(Li et al., 2012)
AU-2	Mackay, Queensland, Australia	-21.1	149.0	2006–2007	Sugarcane	150	no	no	33	38.5	4.7	1.7	9.4	1.61	Automatic chambers	(Denmead et al., 2010)
AU-3	Brisbane, Australia	-26.0	152.0	2007-2009	lychee orchard	256	yes	no	26	37	6.0	2.7	10.1	1.22	automatic chambers	(Rowlings et al., 2013)
AU-4	Queensland, Australia	-27.5	151.8	2009-2011	Cotton; wheat	200	no	yes	76	7	7.2	1.6	11.9	0.46	automated chamber	(Scheer et al., 2012; Scheer et al., 2013; Scheer et al., 2016)
AU-5	Queensland,	-28.2	152.1	2006-2009	wheat	90	yes	no	65	11	6.9	2.0	9.7	0.83	automatic gas sampling	(Wang et al., 2011)

https://doi.org/10.5194/gmd-2021-23
Preprint. Discussion started: 20 April 2021

	d, Australia				wheat										chamber	Scheer et al., 2013; Scheer et al., 2016)
AU-5	Queenslan d, Australia	-28.2	152.1	2006-2009	wheat	90	yes	no	65	11	6.9	2.0	9.7	0.83	automatic gas sampling chambers	(Wang et al., 2011)
AU-6	Wagga, Australia	-35.4	147.5	1993-1994	ryegras s	200	no	no	15.5	74.5	5.5	8.1	9.8	0.087	automatic static chamber	(Galbally et al., 2010)
AF-1	Kaptumo, Kenya	0.12	35.5	2013-2014	vegetab le	110	yes	no	27.8	62.3	6.0	4.1	12.4	0.25	static chamber	(Rosenstock et al., 2016)
AF-2	Kenya	-0.31	35.4	2015-2016	tea	150	no	no	59	20	3.9		12.4	0.34	static chamber method	(Wanyama et al., 2018)
SA-1	Ariquemes , Rondnia State, Brazil	-10.5	-52.5	2001-2002	B.briza ntha	42	yes	no	23.5	71	5.3	6.0	9.6	0.89	recirculating chamber	(Passianoto et al., 2003)
SA-2	Santa Maria, Brazil	-29.7	-53.7	2010-2011	Maize and wheat	125	no	yes	19.2	44.3	5.9		11.1	1.66	non-steady-state chambers	(Aita et al., 2015)
SA-3	Campinas, Brazil	-22.9	-47.1	2011-2013	Sugarc ane	120	yes	no	41	41.5	5.6	5.8	10.8	0.68	PVC static chambers	(Soares et al., 2015)

https://doi.org/10.5194/gmd-2021-23
Preprint. Discussion started: 20 April 2021

https://doi.org/10.5194/gmd-2021-23
Preprint. Discussion started: 20 April 2021

Geoscientific Model Development Discussions

960

Table 3. List of calibrated values for COE_{dNO3} and the model performance indices for calibrated sites

ID	latitude	longitude	COE_{dNO3}	*D*-value	*RMSE*	*R*	counts
NA-1	42.08	-82.57	0.05	0.65	1.16	0.44	53
NA-2	44.75	-93.06	0.01	0.56	1.09	0.35	106
NA-3	39.43	-77.30	0.03	0.69	3.60	0.57	157
NA-4	45.92	-66.60	0.04	0.81	0.92	0.84	50
NA-5	46.80	-71.38	0.03	0.81	3.66	0.68	53
NA-6	40.65	-104.98	0.03	0.84	0.90	0.73	123
NA-7	30.35	-91.17	0.04	0.59	4.09	0.40	43
NA-8	38.30	-121.47	0.029	0.61	1.87	0.48	135
NA-9	49.24	-121.76	0.01	0.75	0.92	0.84	57
AS-1	28.23	77.20	0.02	0.69	0.54	0.48	123
AS-2	43.50	124.80	0.025	0.50	1.73	0.25	170
AS-3	31.26	105.49	0.01	0.67	1.35	0.51	149
AS-4	32.06	118.96	0.03	0.64	2.12	0.56	73
AS-5	34.93	110.71	0.03	0.86	0.82	0.83	373
AS-6	35.00	114.34	0.025	0.81	0.86	0.69	76
AS-7	36.05	140.08	0.025	0.78	0.33	0.63	284
AS-8	36.90	117.90	0.01	0.76	2.01	0.58	133
AS-9	29.88	114.28	0.01	0.65	0.31	0.49	41
AS-10	41.58	60.52	0.025	0.74	6.03	0.60	93
EU-1	52.44	13.01	0.02	0.54	2.57	0.29	361
EU-2	46.42	0.12	0.04	0.51	0.72	0.32	579
EU-3	59.57	30.13	0.02	0.52	1.31	0.33	107
EU-4	31.98	34.84	0.02	0.61	30.19	0.54	76
EU-5	52.60	20.27	0.01	0.75	0.30	0.62	57
EU-6	51.18	0.95	0.05	0.79	4.37	0.76	45
EU-7	48.72	9.19	0.025	0.77	1.46	0.66	101
EU-8	40.62	14.97	0.04	0.87	0.23	0.76	142
EU-9	40.53	-3.28	0.04	0.91	1.36	0.88	64
AU-1	-31.6	117.22	0.015	0.47	0.12	0.25	226
AU-2	-21.08	148.99	0.028	0.69	5.15	0.52	130
AU-3	-26.00	152.00	0.025	0.80	2.00	0.75	536
AU-4	-27.52	151.78	0.023	0.47	1.27	0.27	294
AU-5	-28.2	152.10	0.01	0.72	0.65	0.56	136
AU-6	-35.38	147.50	0.01	0.46	0.20	0.35	69
AF-1	0.10	35.48	0.01	0.92	0.23	0.94	52
AF-2	-0.31	35.39	0.012	0.87	0.65	0.93	75
SA-1	-10.50	-52.50	0.05	0.93	0.70	0.90	40
SA-2	-29.72	-53.72	0.049	0.81	4.19	0.67	60
SA-3	-22.87	-47.07	0.035	0.74	1.25	0.65	98

https://doi.org/10.5194/gmd-2021-23
Preprint. Discussion started: 20 April 2021

Geoscientific Model Development Discussions
Open Access
EGU

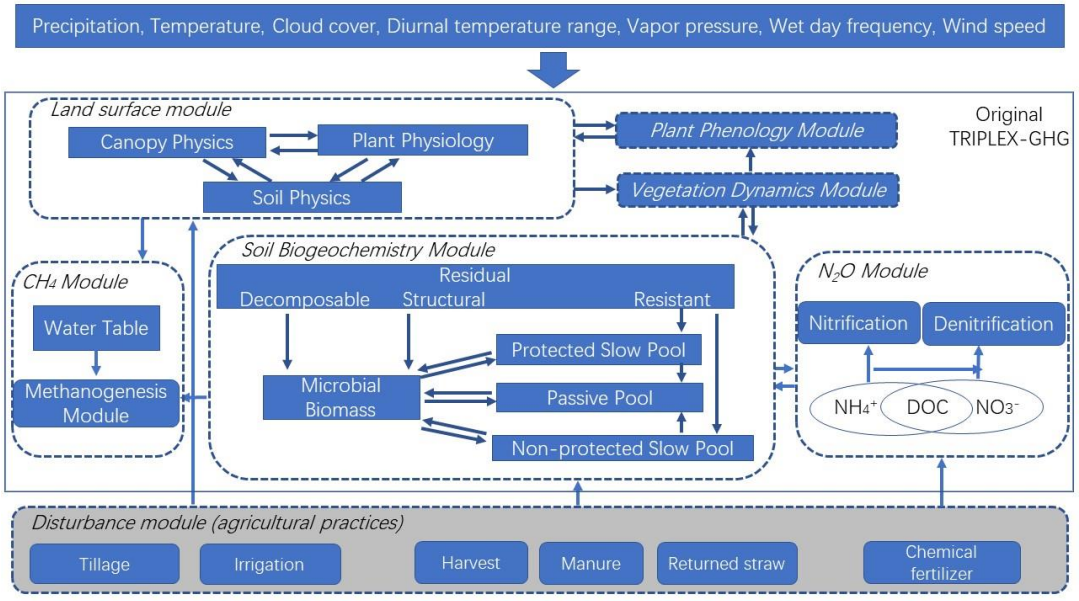

Fig. 1 Model's structural concept and integration of agricultural practices into the TRIPLEX-GHG (revised from Zhang et al. (2017)). The rectangular insert with the light grey background represents the different agricultural practices and how they interact with the other submodules (e.g., the land surface module).

.

https://doi.org/10.5194/gmd-2021-23
Preprint. Discussion started: 20 April 2021

Geoscientific Model Development Discussions

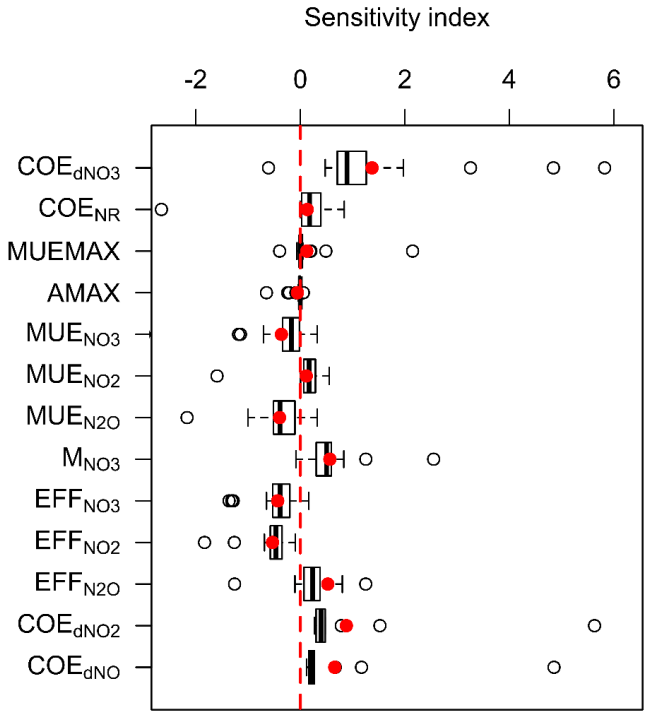

Fig. 2 Sensitivity analysis of the different parameters. The closed red dots show the mean sensitivity index value of the parameters.
970 **The outliers are shown as open dots.**

https://doi.org/10.5194/gmd-2021-23
Preprint. Discussion started: 20 April 2021

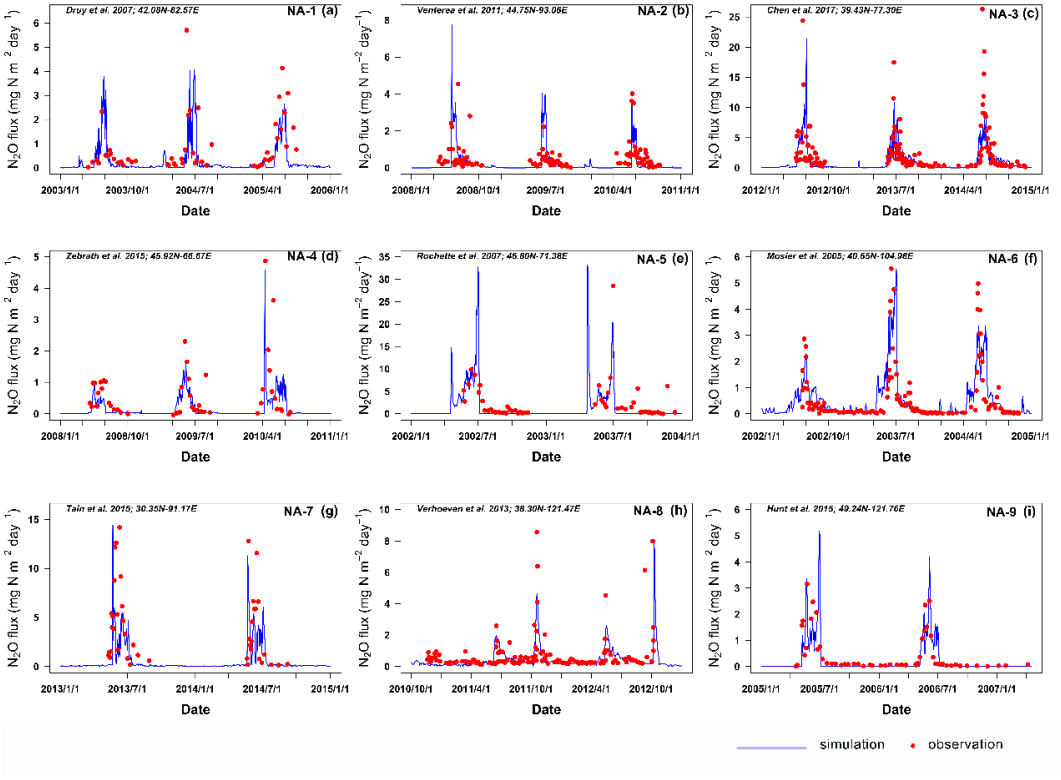

Figure 3. Comparison of the modeled and observed N_2O emissions from the cropland sites located in North America.

https://doi.org/10.5194/gmd-2021-23
Preprint. Discussion started: 20 April 2021

Geoscientific Model Development Discussions

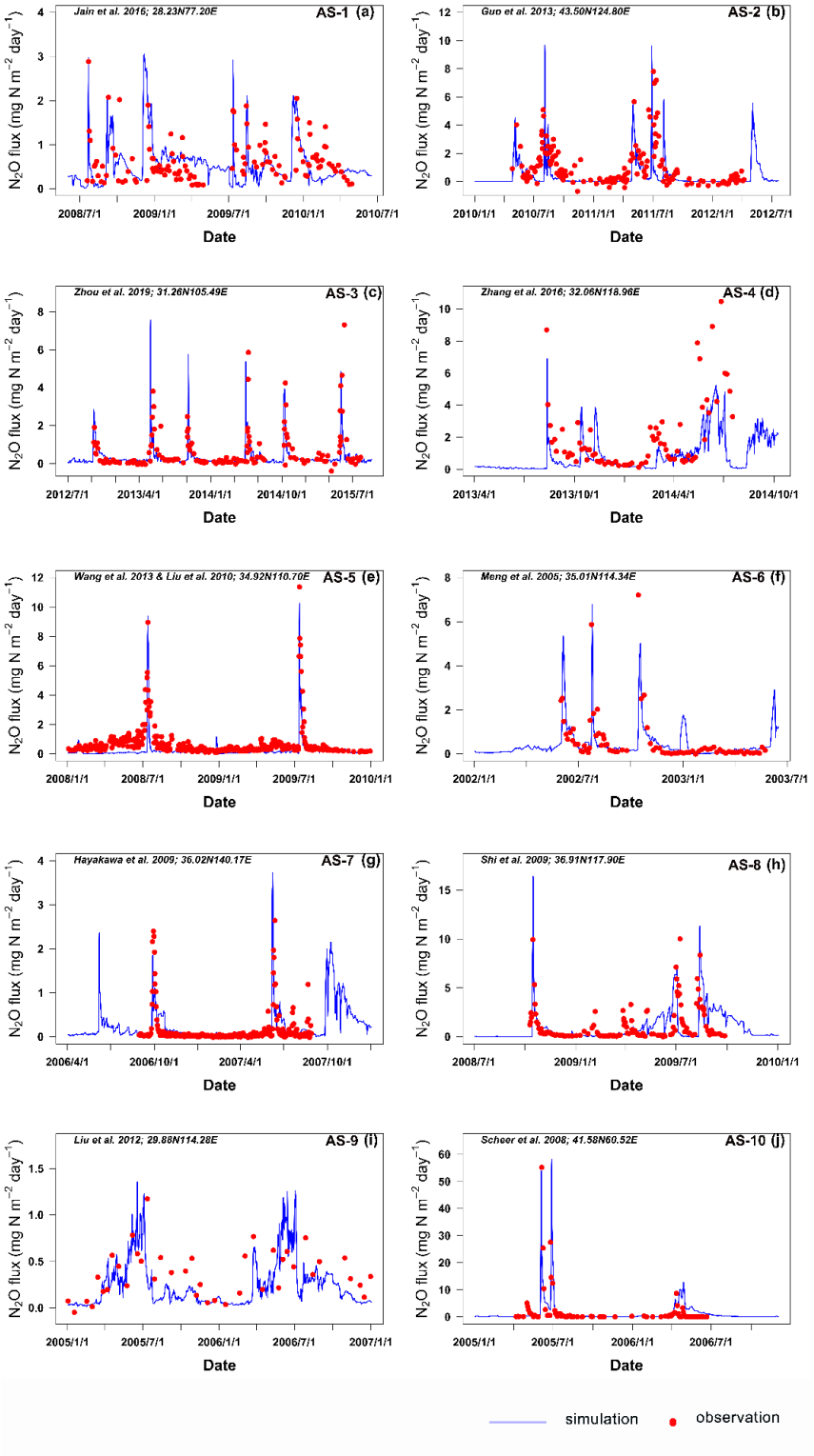

975 **Figure 4. Comparison of the modeled and observed N_2O emissions from the cropland sites located in Asia.**

https://doi.org/10.5194/gmd-2021-23
Preprint. Discussion started: 20 April 2021

Geoscientific Model Development Discussions

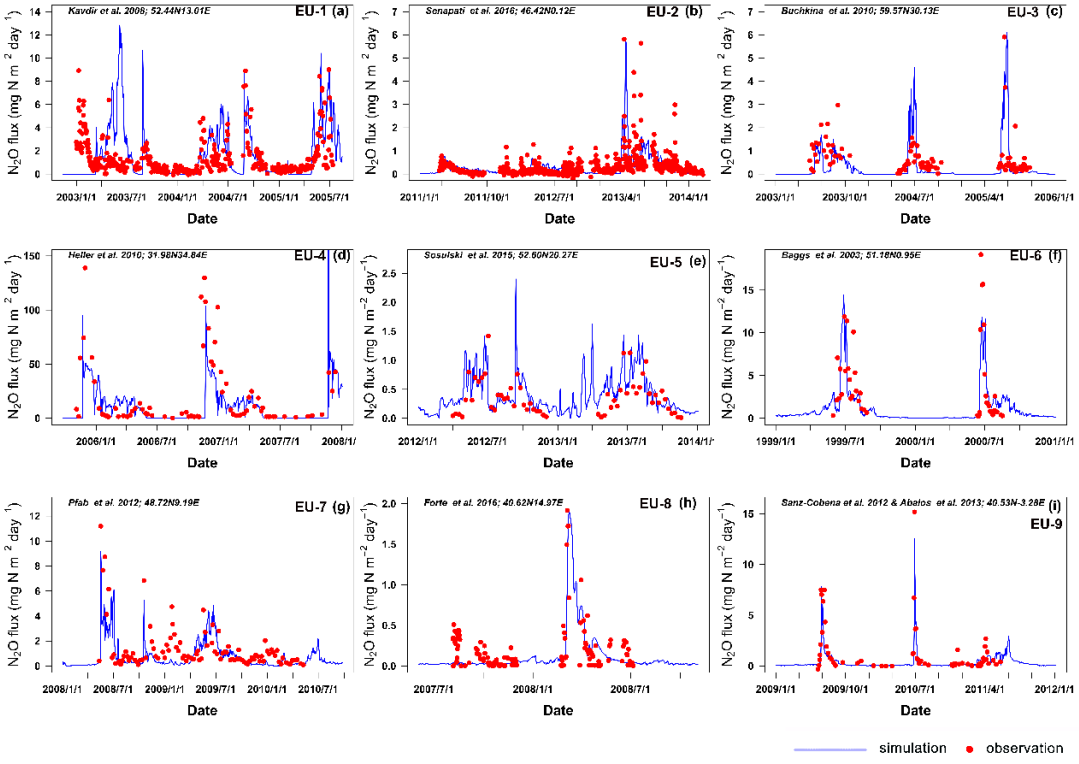

Figure 5. Comparison of the modeled and observed N_2O emissions from the cropland sites located in Europe.

980

https://doi.org/10.5194/gmd-2021-23
Preprint. Discussion started: 20 April 2021

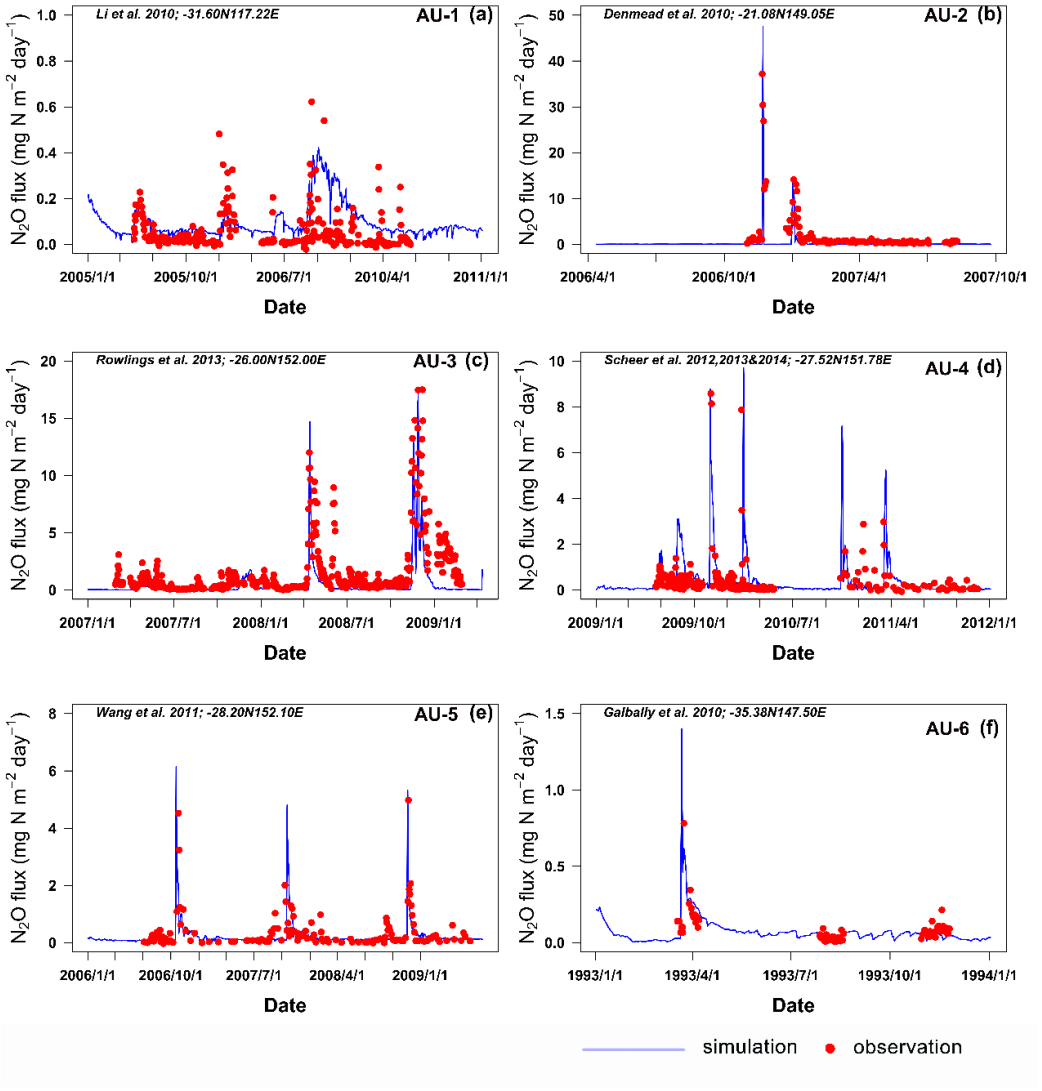

Figure 6. Comparison of the modeled and observed N_2O emissions from the cropland sites located in Australia.

https://doi.org/10.5194/gmd-2021-23
Preprint. Discussion started: 20 April 2021

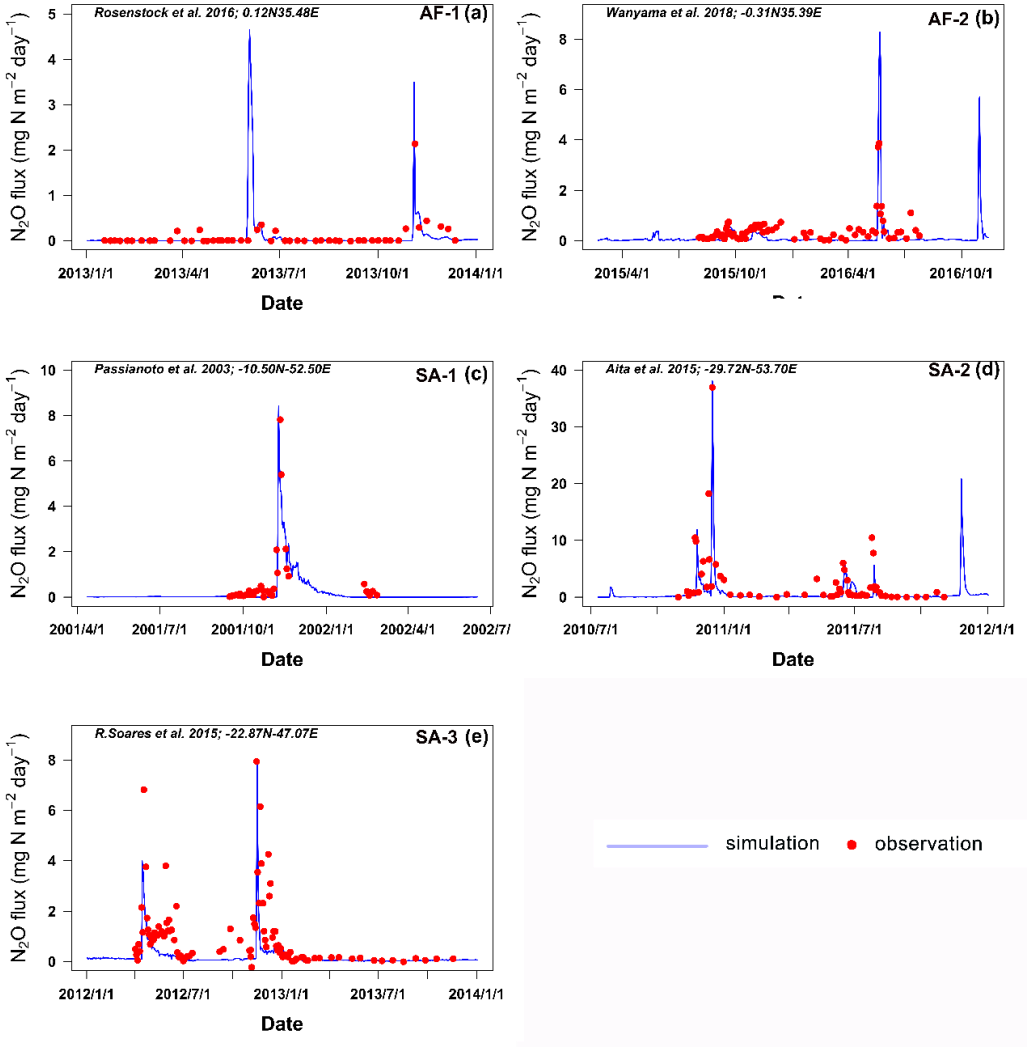

985

Figure 7. Comparison of the modeled and observed N_2O emissions from the cropland sites located in Africa and South America.

https://doi.org/10.5194/gmd-2021-23
Preprint. Discussion started: 20 April 2021

Geoscientific Model Development Discussions

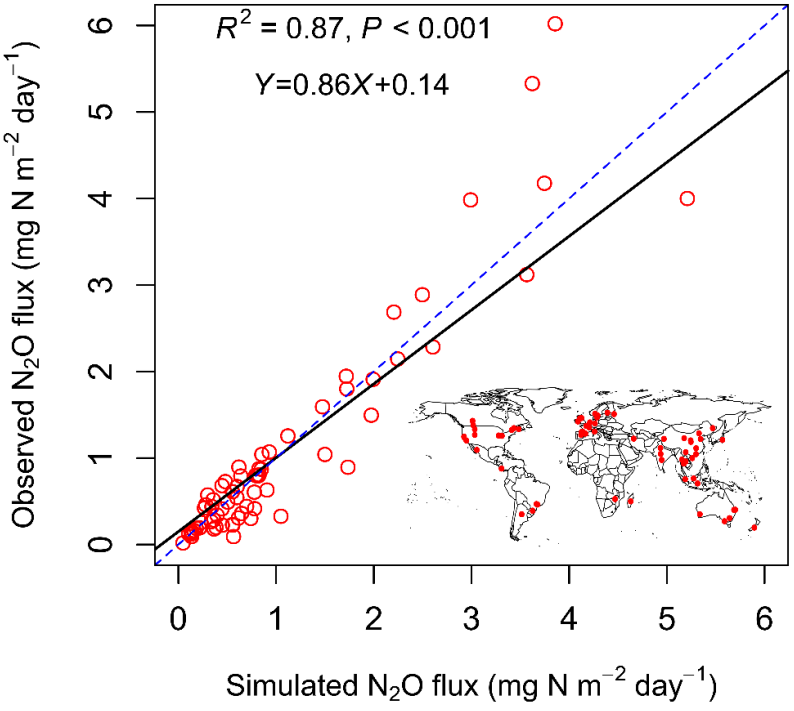

990 **Fig. 8. Comparison of the measured and modeled N_2O emissions from the validation sites (open red dots) and their global distribution (closed red dots on map).**